Searches for Gravitational Wave Background and Future Prospects

on behalf of the LIGO-Virgo-KAGRA collaboration

Jishnu Suresh

Henri Poincaré Fellow,

ARTEMIS, Observatoire de la Côte d'Azur, Nice

ARTEMIS

OBSERVATOIRE DE LA CÔTE D'AZUR — UNIVERSITÉ CÔTE D'AZUR —

GRAVITATIONAL WAVE SPECTRA

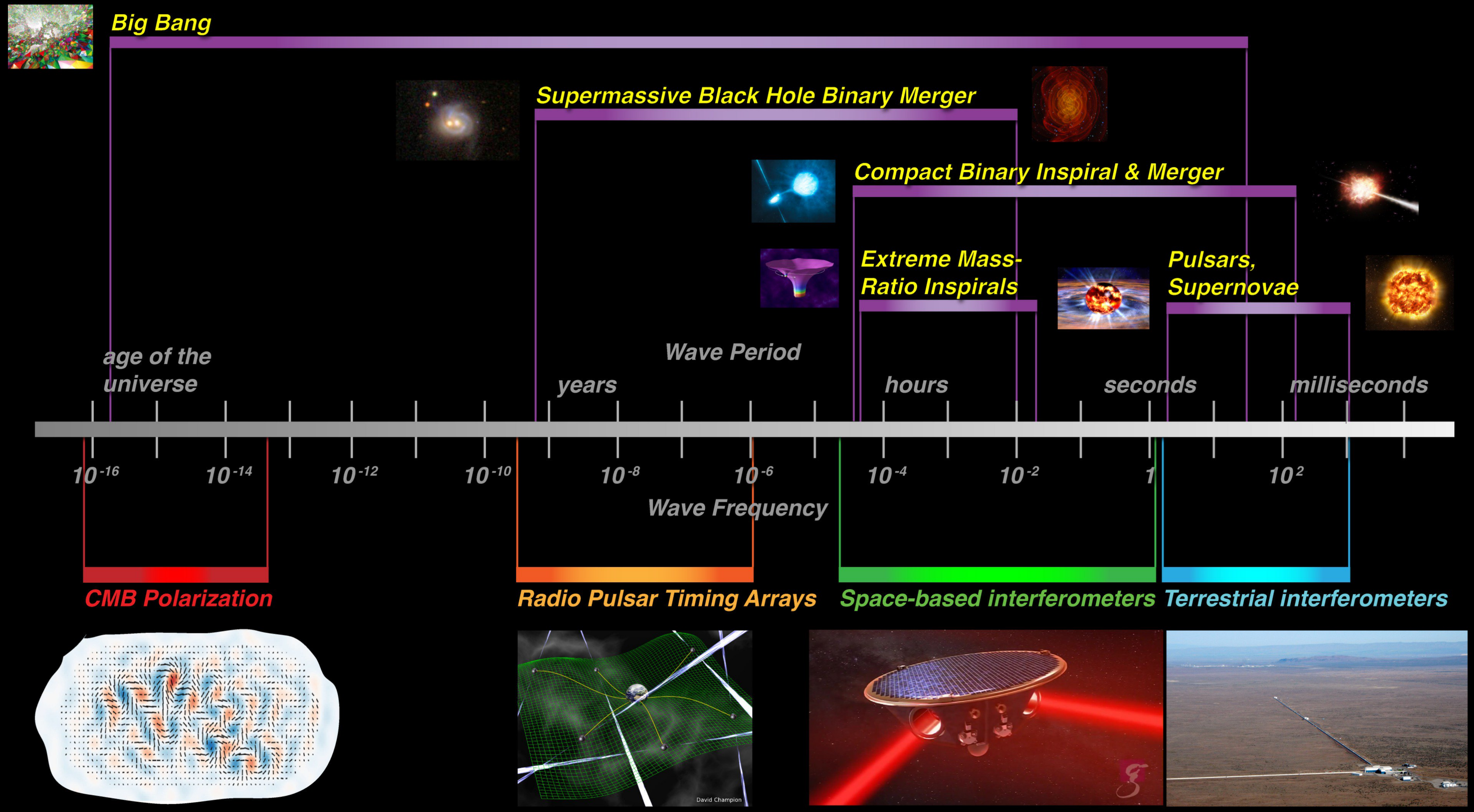

credit: NASA/J. I.Thorpe

GRAVITATIONAL WAVE SPECTRA

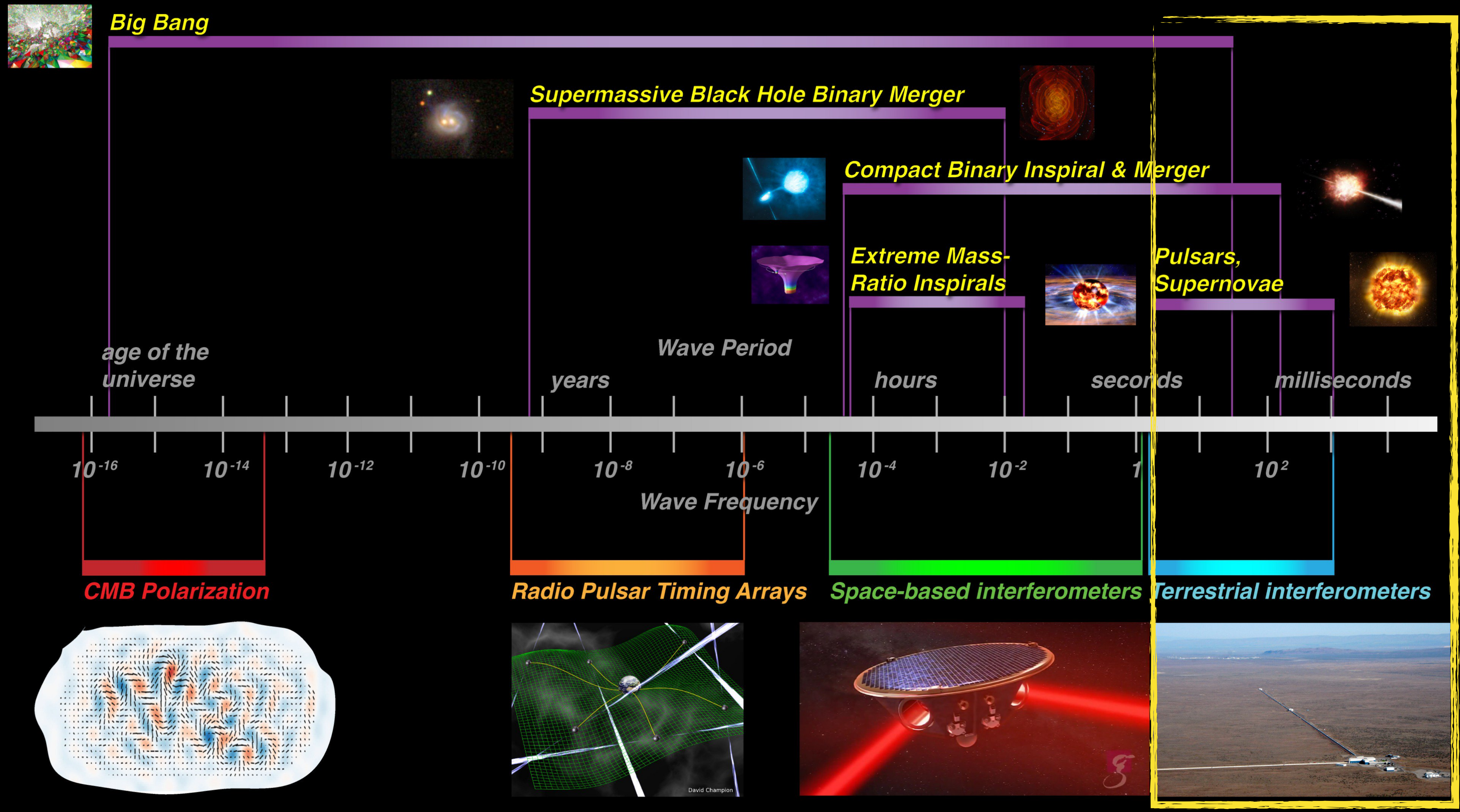

credit: NASA/J. I.Thorpe

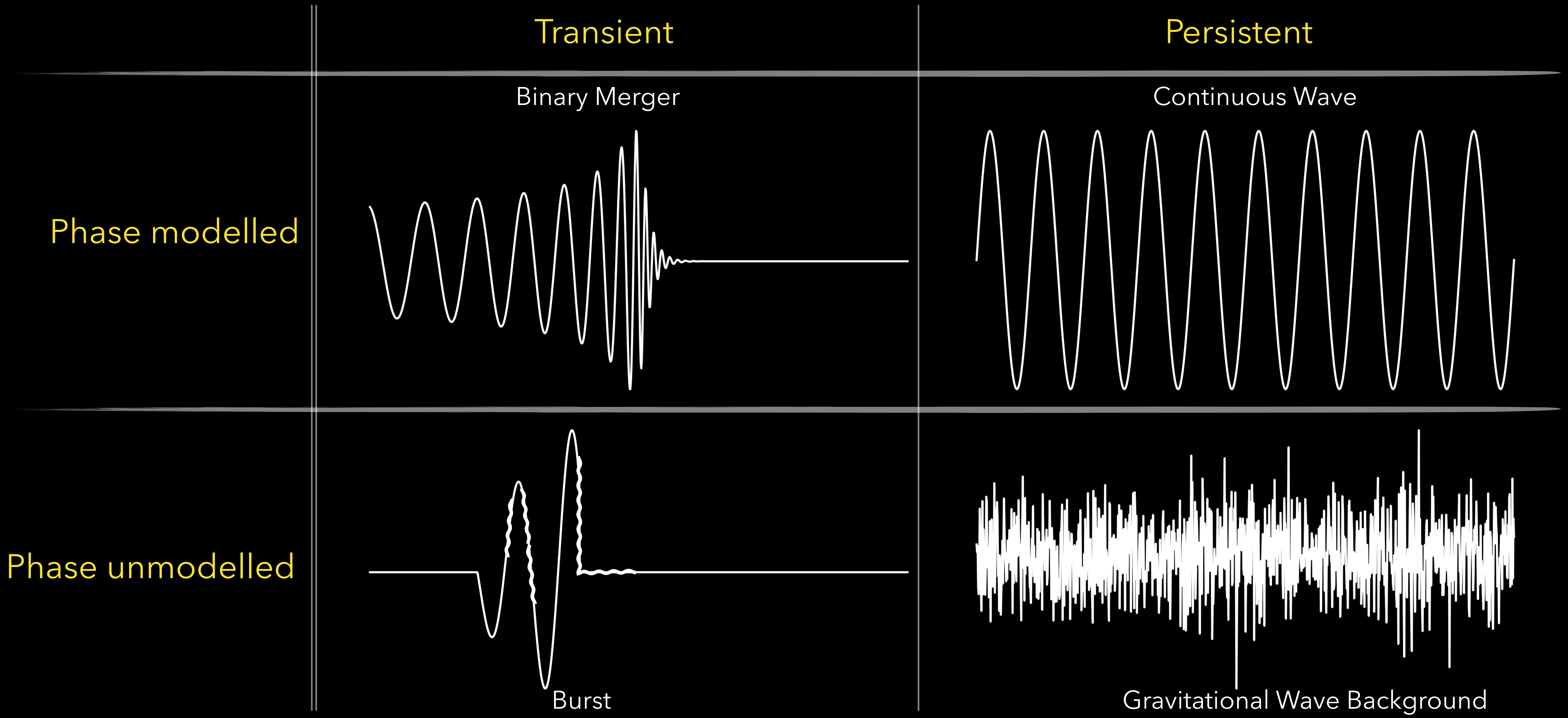
Transient
Persistent
Phase modelled
Phase unmodelled
Binary Merger
Continuous Wave
Burst
Gravitational Wave Background

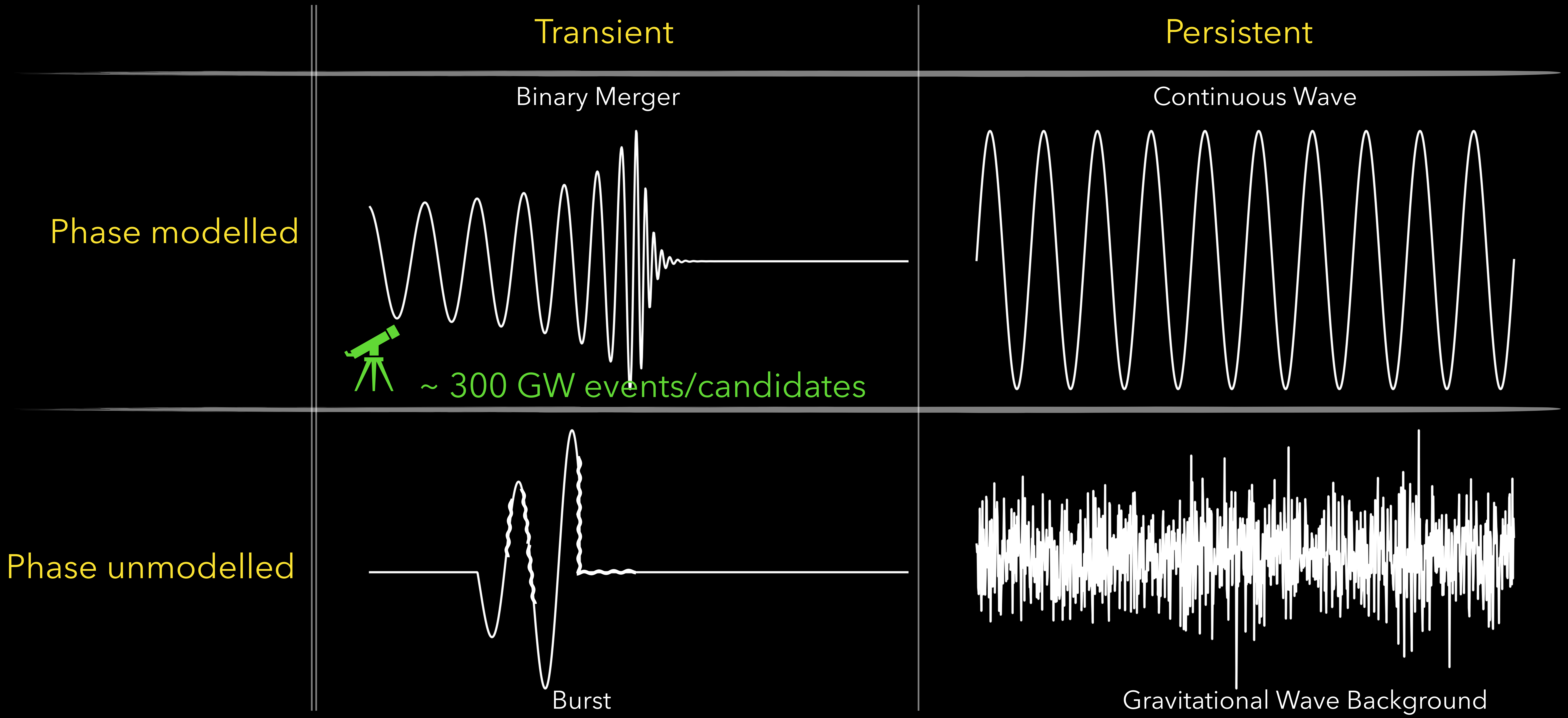
Transient
Persistent
Binary Merger
Continuous Wave
Phase modelled
~ 300 GW events/candidates
Phase unmodelled
Burst
Gravitational Wave Background

OPERATIONAL DEFINITION

Superposition of signals too weak or too numerous to individually detect

Looks like noise in a single detector

Characterized statistically in terms of ensemble averages of the metric perturbations

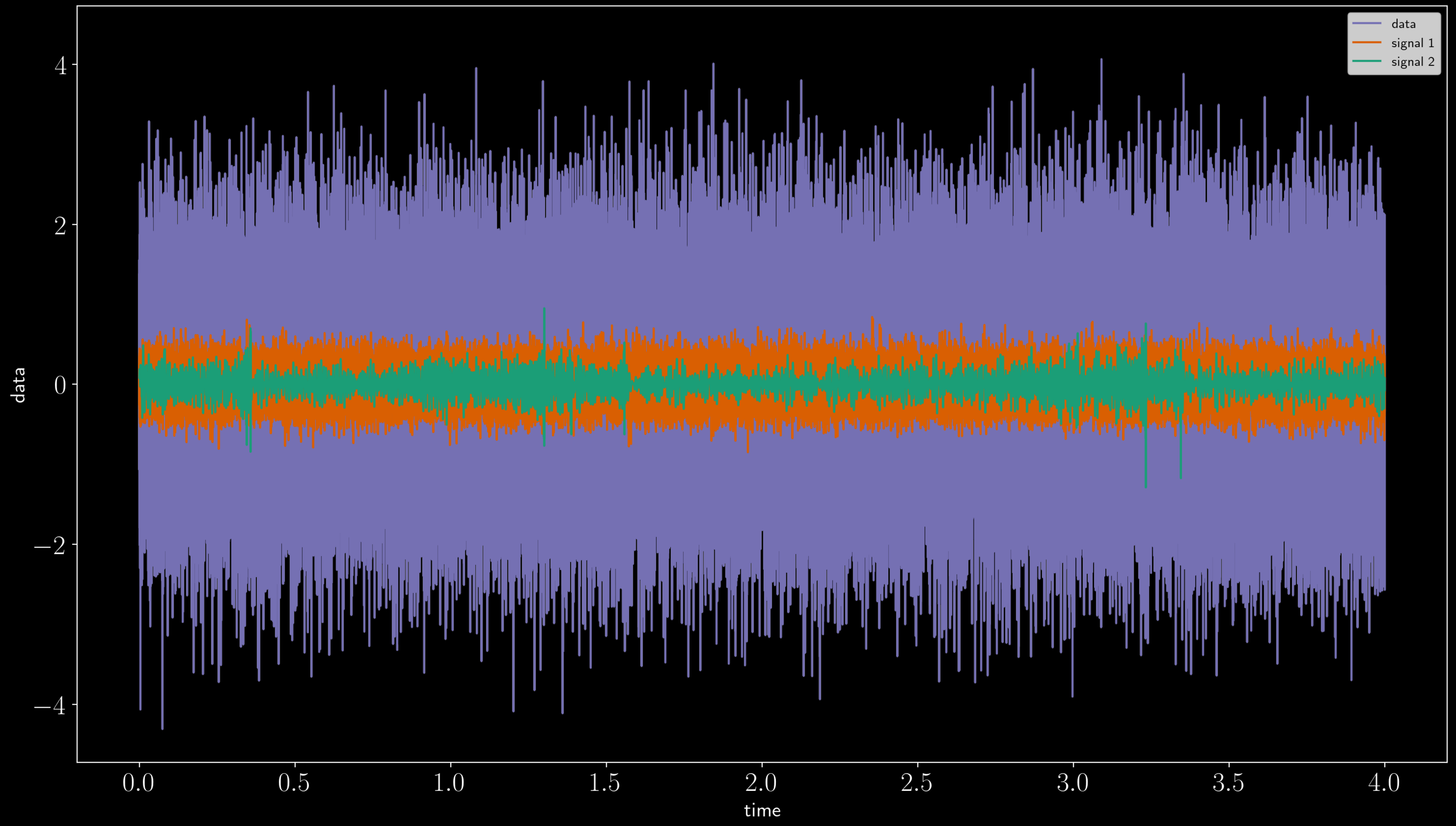

TYPES OF GRAVITATIONAL WAVE BACKGROUND

(1) Spatial distribution

isotropic

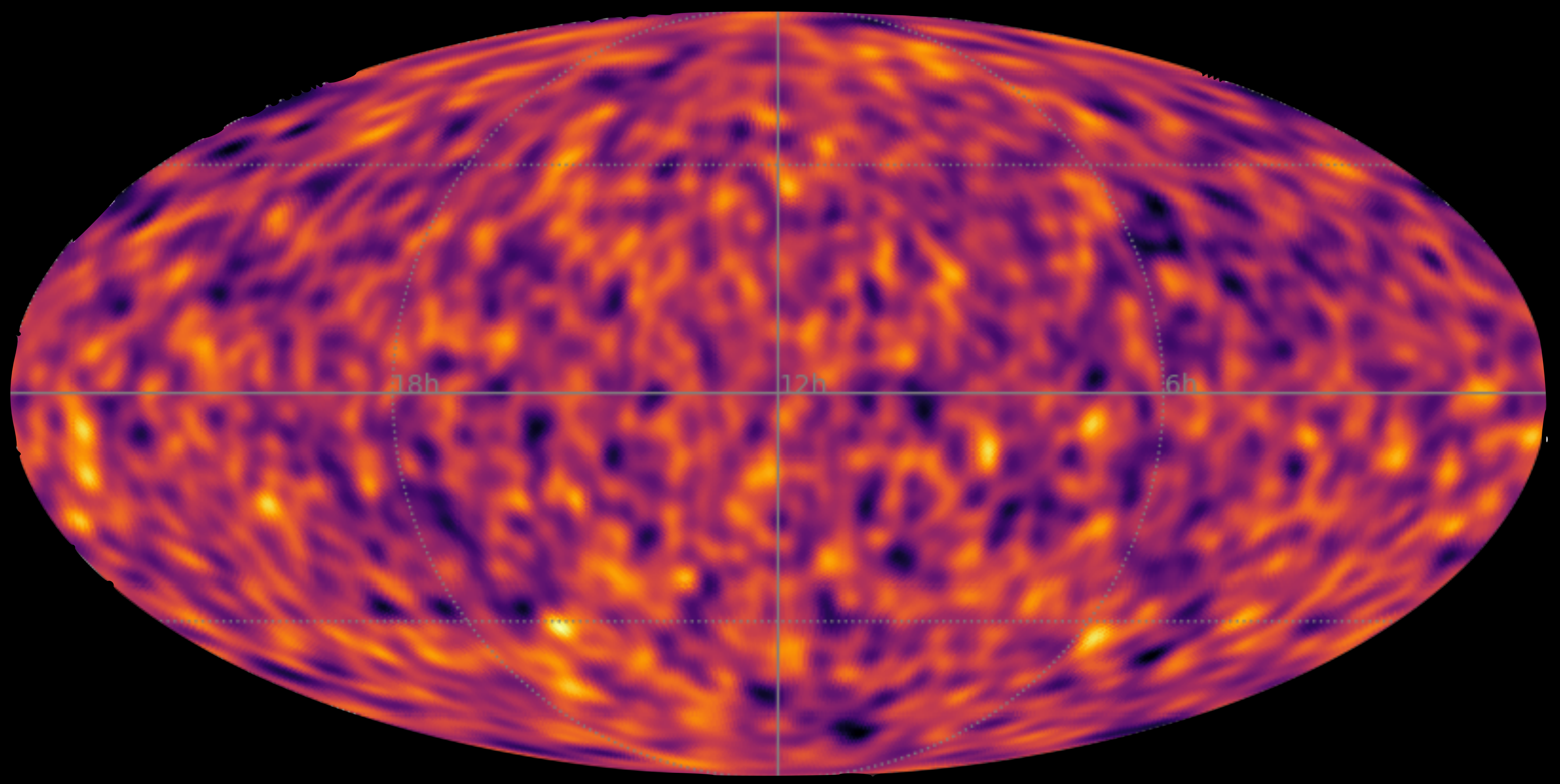

anisotropic

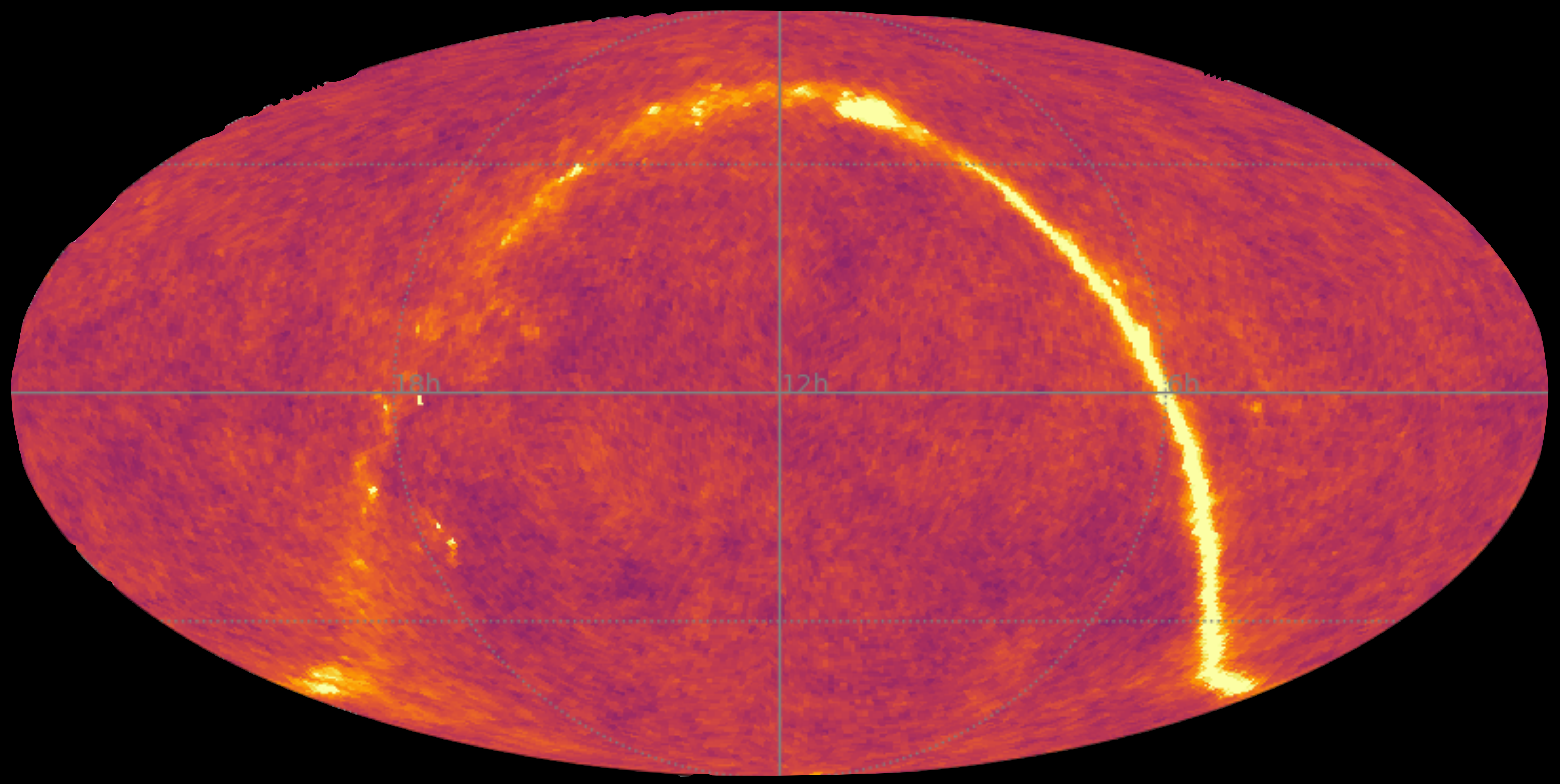

TYPES OF GRAVITATIONAL WAVE BACKGROUND

(2) Temporal distribution

Stationary Gaussian

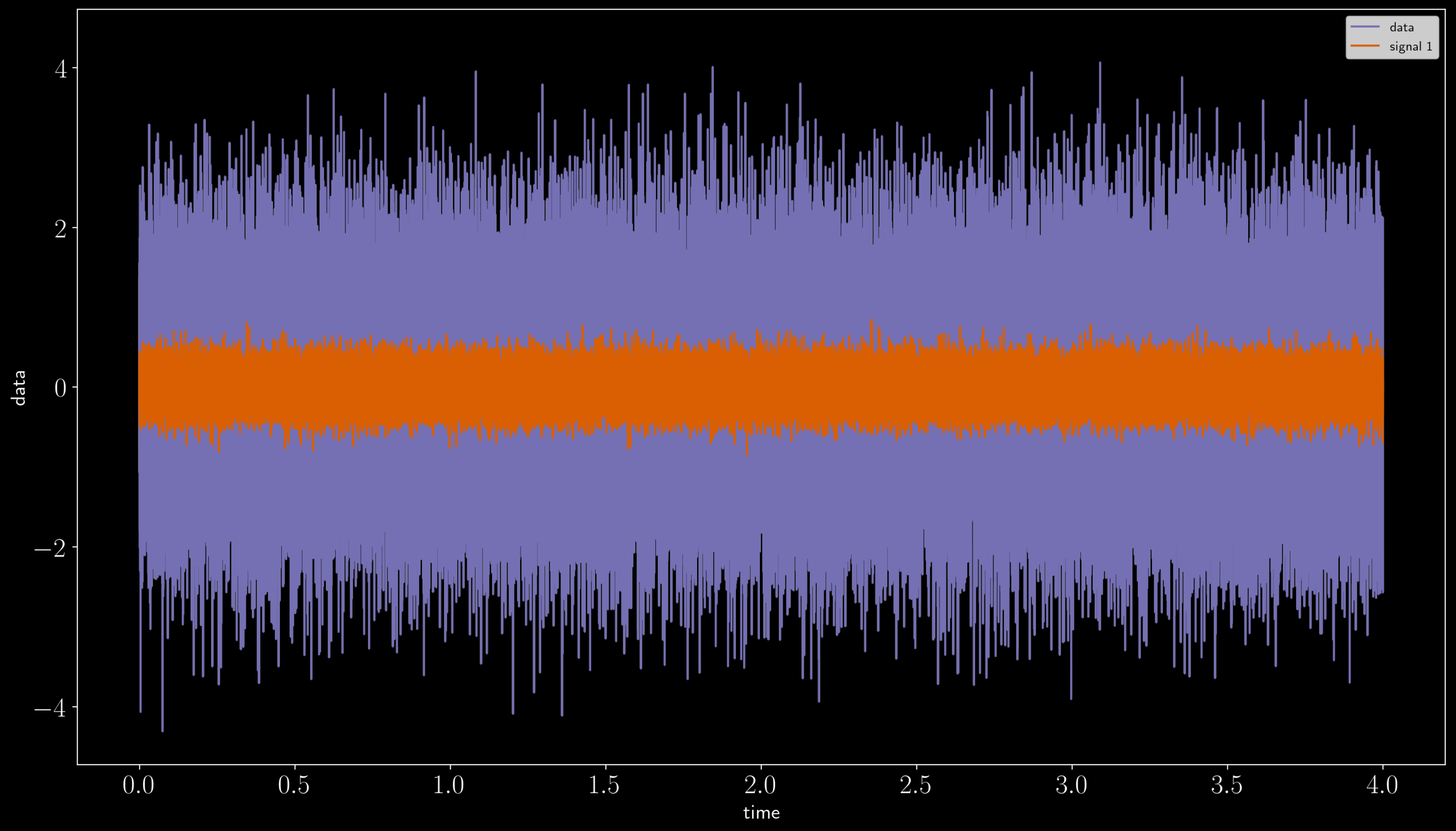

Non-stationary (non-gaussian)

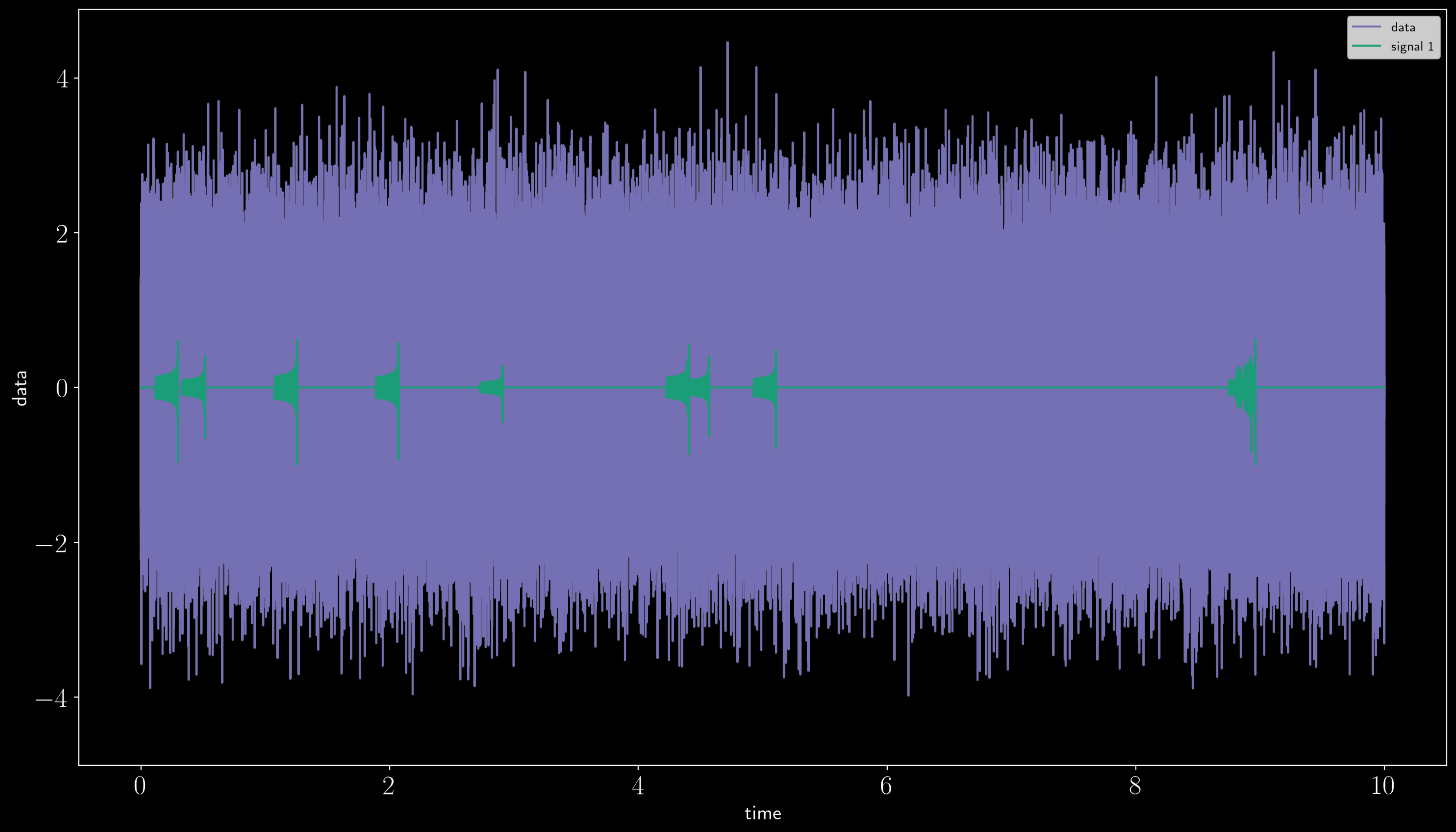

GRAVITATIONAL WAVE BACKGROUND

In this talk, we will only consider the following cases

Unpolarized,

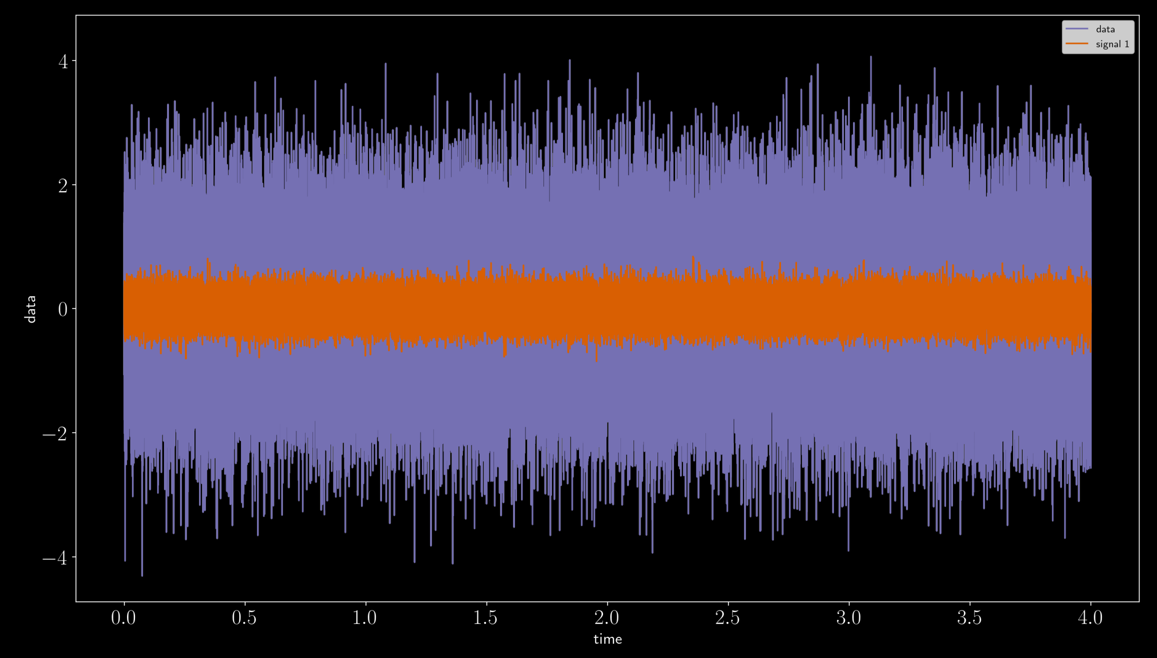

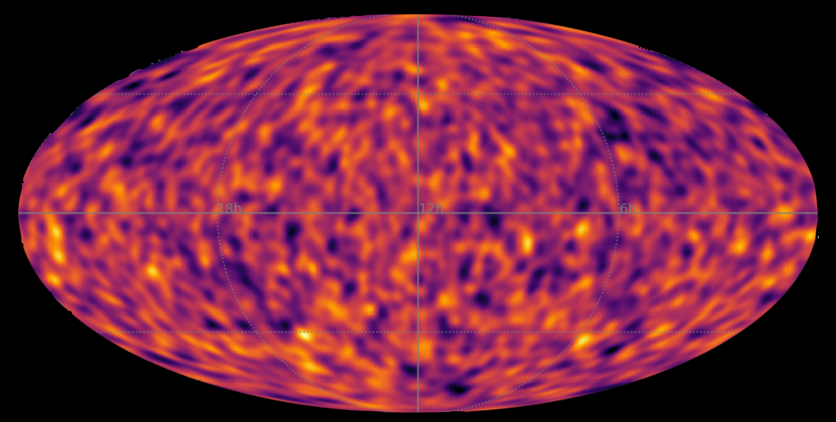

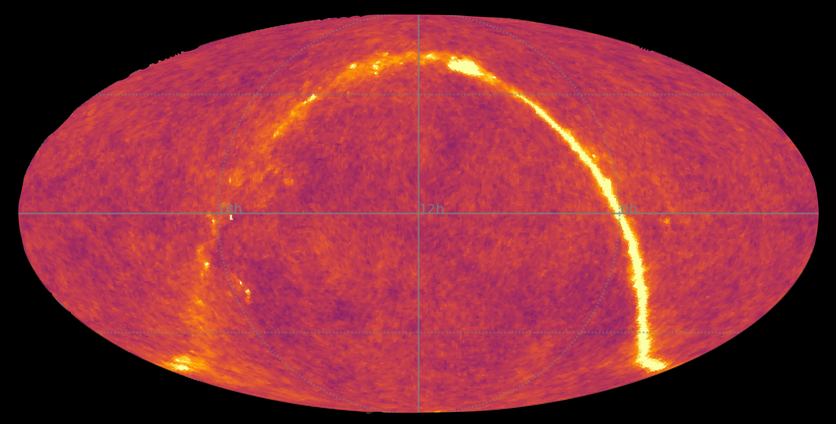

Unpolarized, stationary, isotropic:

$$\langle h_A(f,\hat{n})\, h^*_{A'}(f',\hat{n}')\rangle = \frac{1}{16\pi} S_h(f)\, \delta(f-f')\delta_{AA'}\,\delta^2(\hat{n},\hat{n}')$$

Unpolarized, stationary, anisotropic:

$$\langle h_A(f,\hat{n})\, h^*_{A'}(f',\hat{n}')\rangle = \frac{1}{4}\mathscr{P}(f,\hat{n})\, \delta(f-f')\delta_{AA'}\,\delta^2(\hat{n},\hat{n}')$$

where $S_h(f) = \frac{3H_0^2}{2\pi^2}\frac{\Omega_{\rm gw}(f)}{f^3}$

WHICH GWBs WE ARE SENSITIVE TO?

	Cosmological Origin	Astrophysical Origin
EM	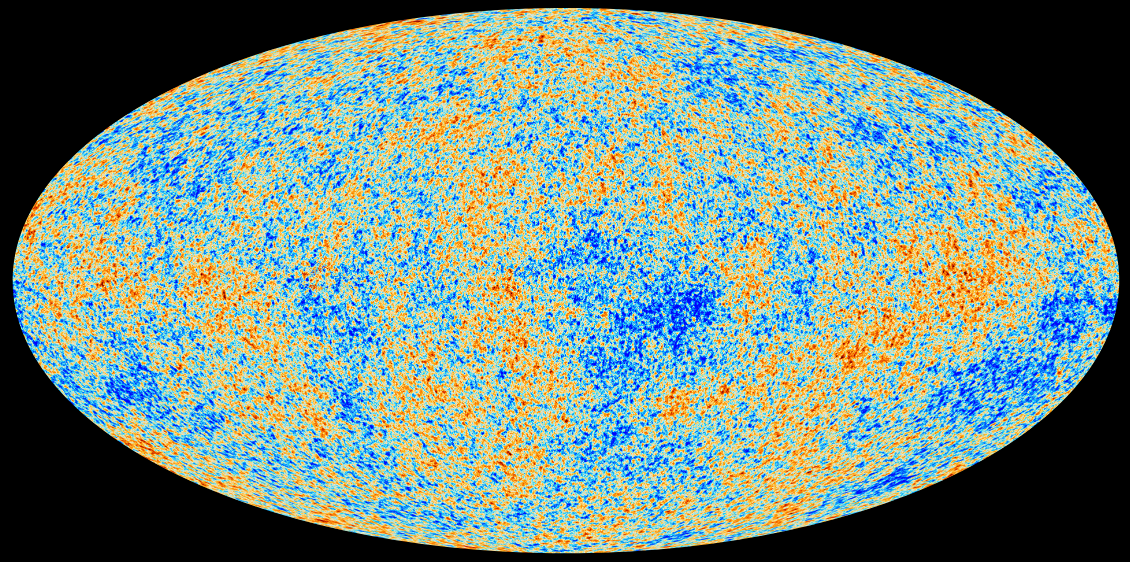 PLANCK CMB MAP	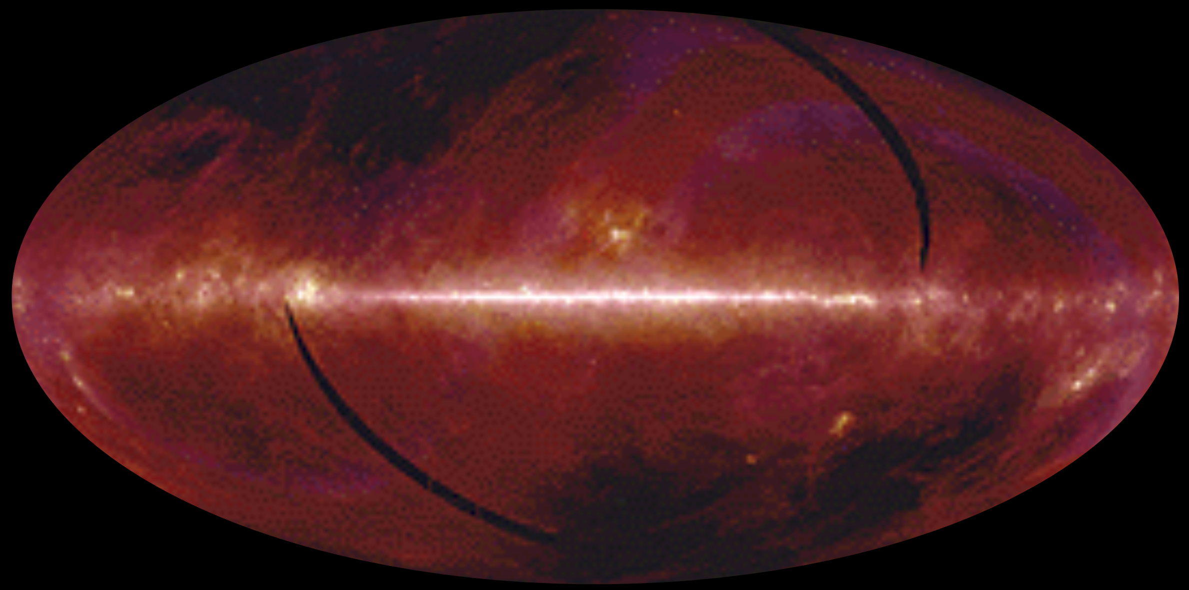 PLANCK IR MAP
GW	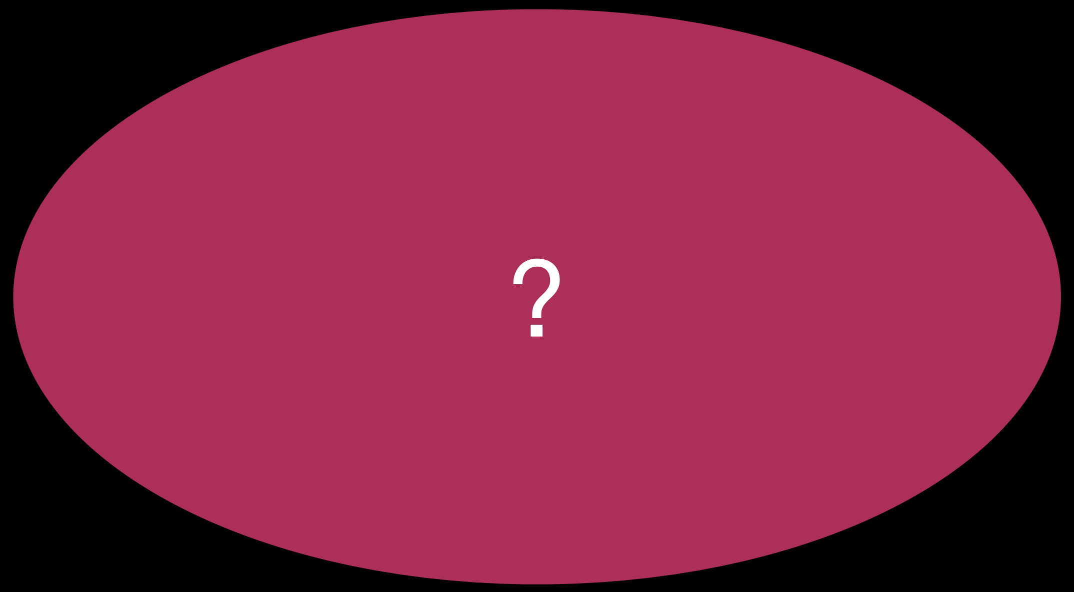 COSMOLOGICAL GWB	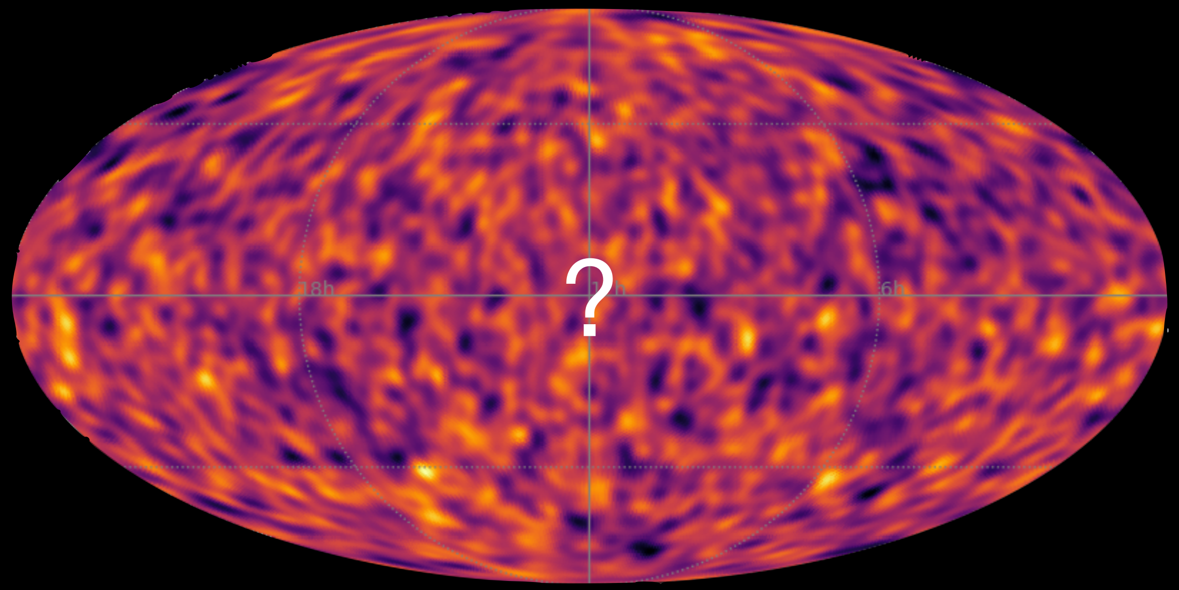 ASTROPHYSICAL GWB

WHICH GWBs WE ARE SENSITIVE TO?

Astrophysical Origin

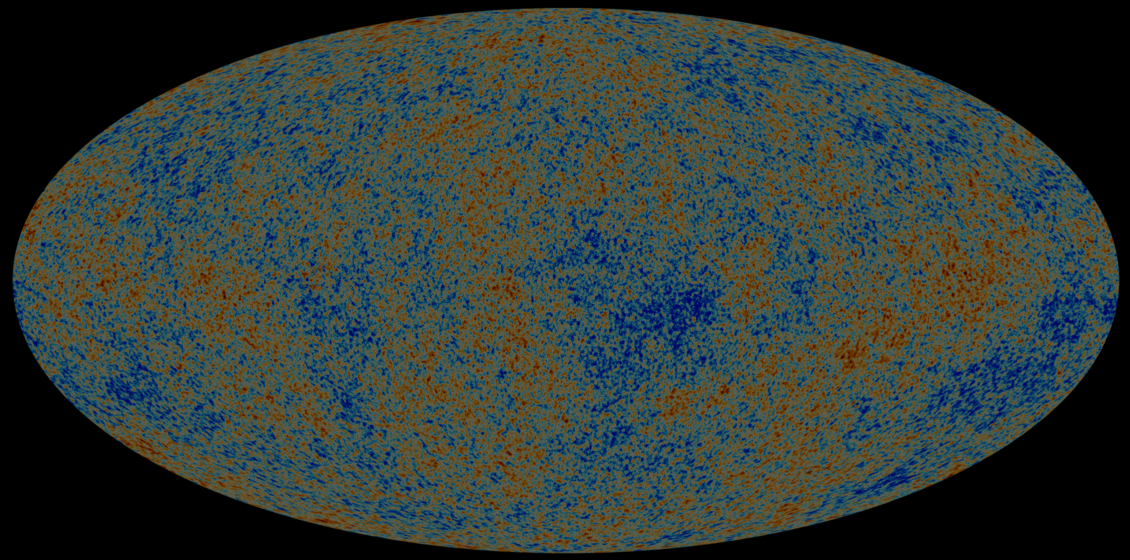

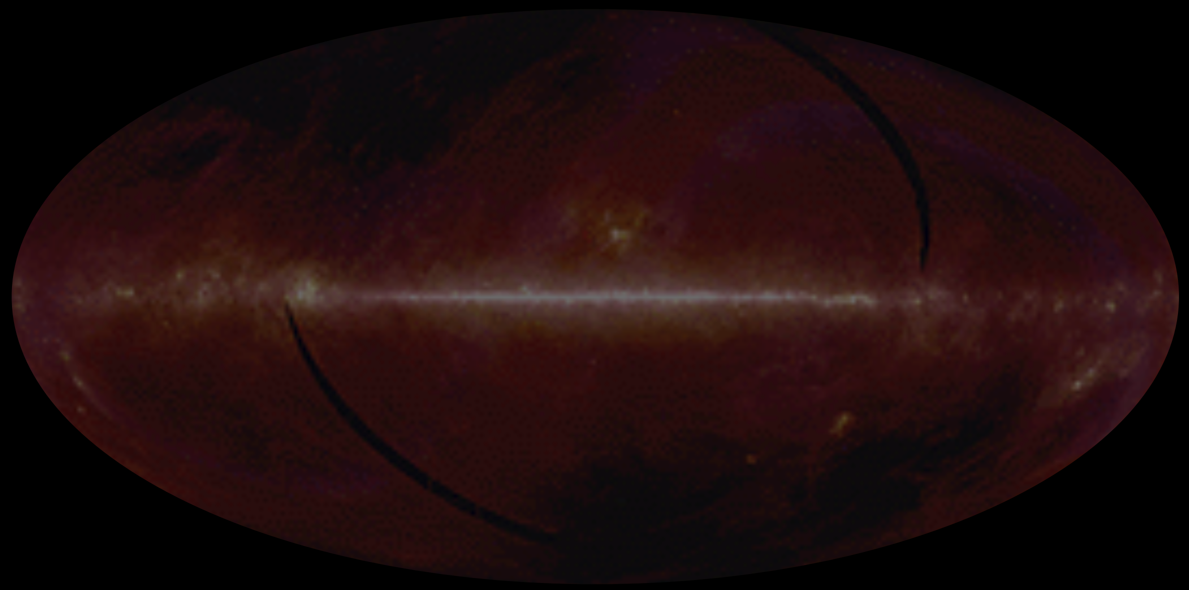

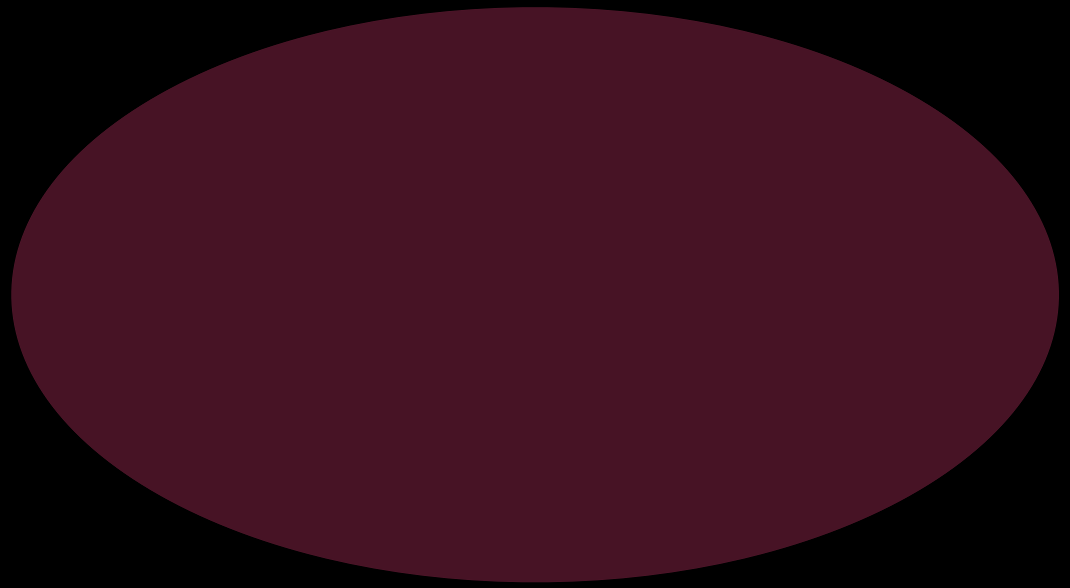

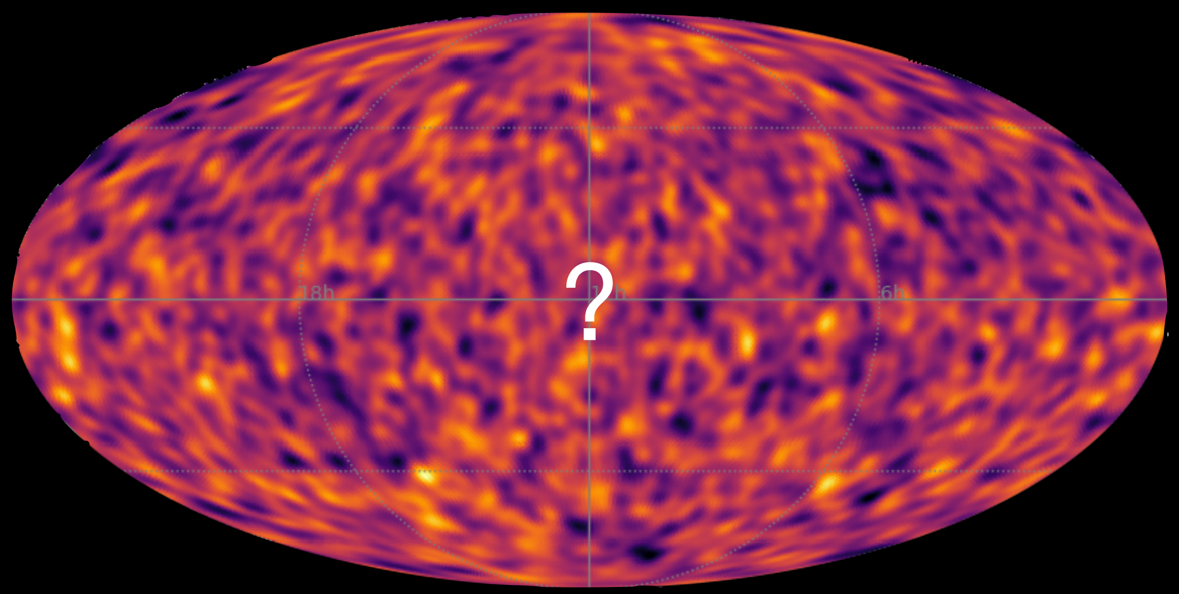

ASTROPHYSICAL GWB

ASTROPHYSICAL GWB

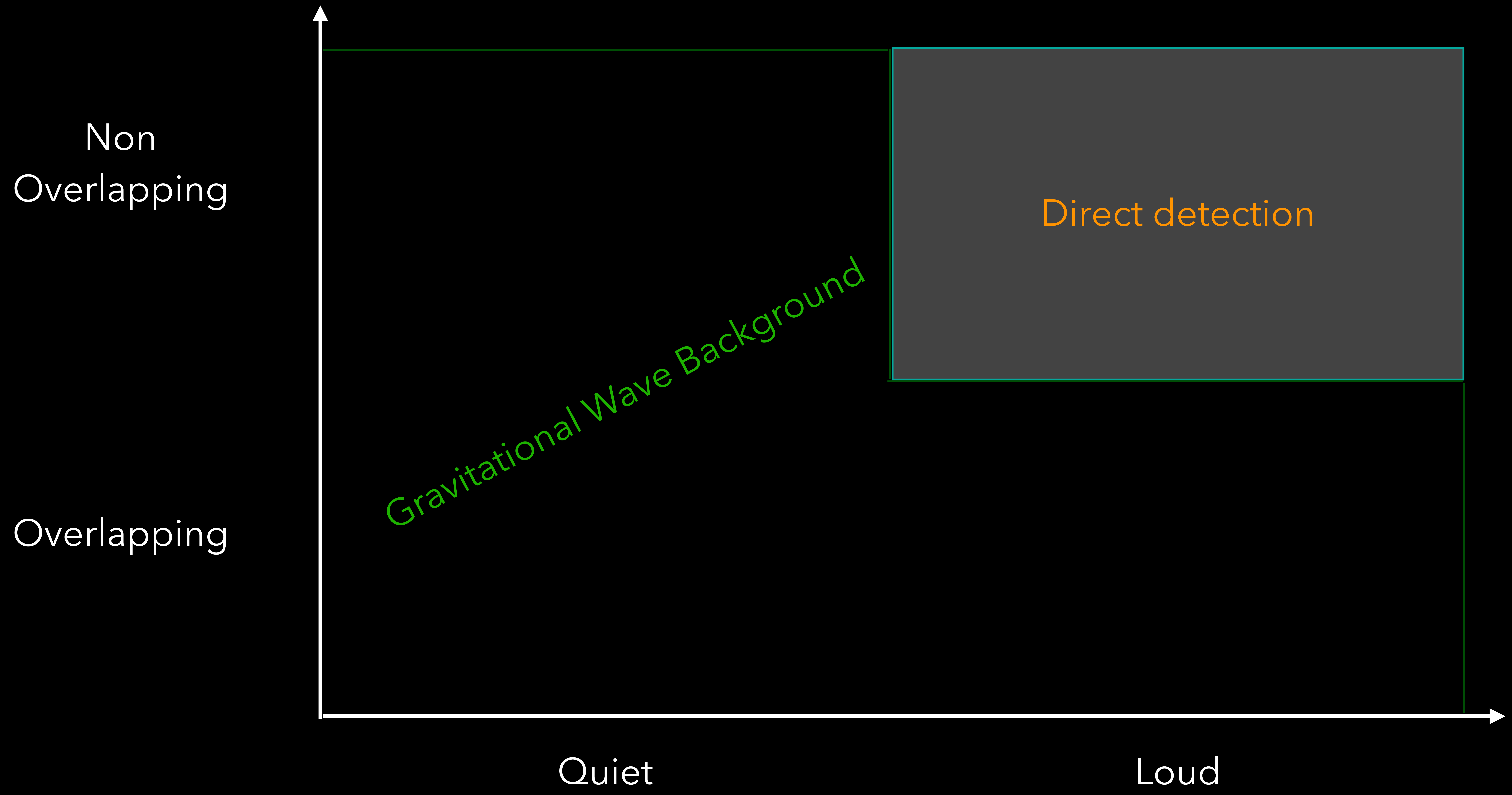

ASTROPHYSICAL GWB

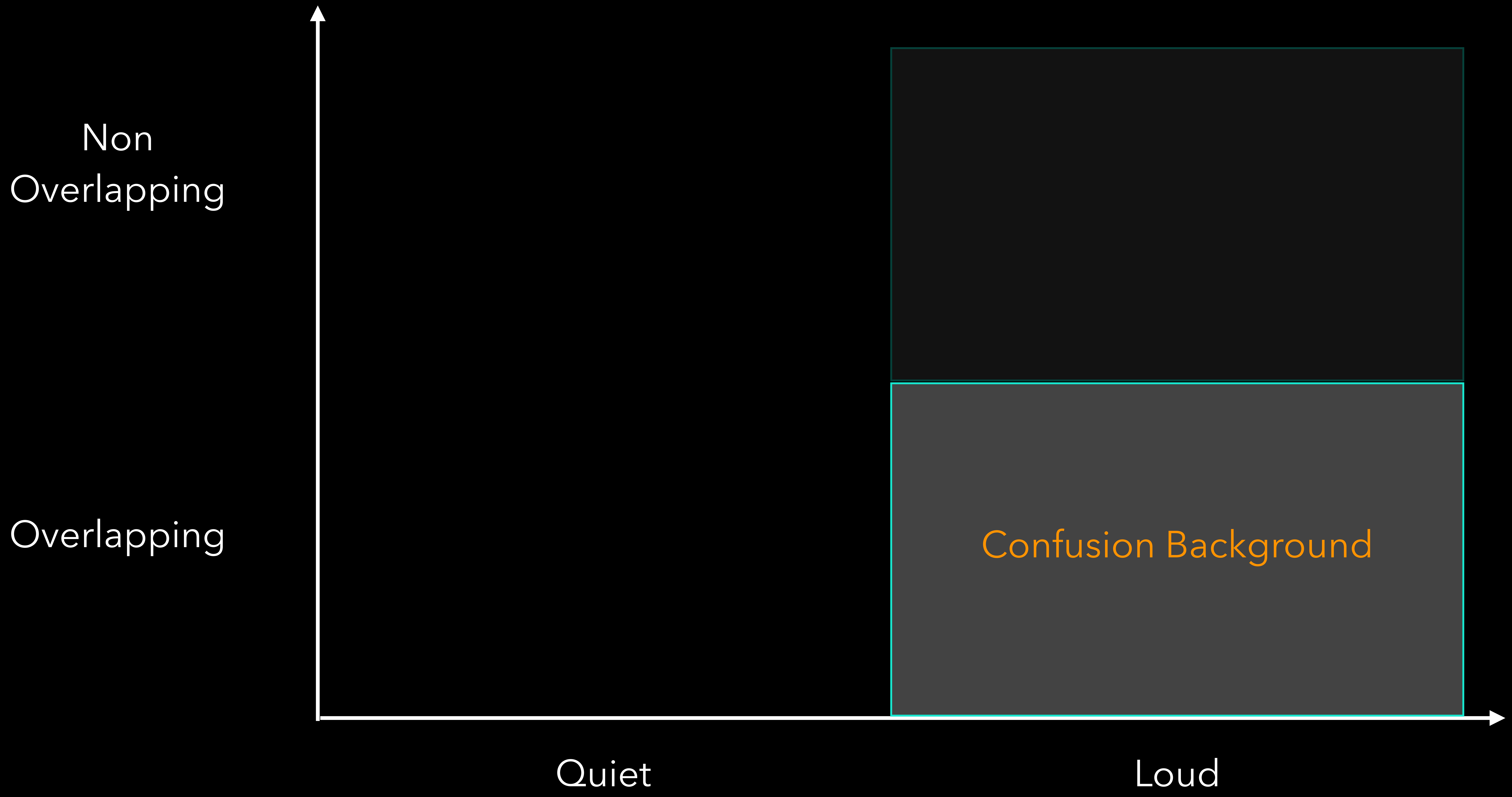

ASTROPHYSICAL GWB

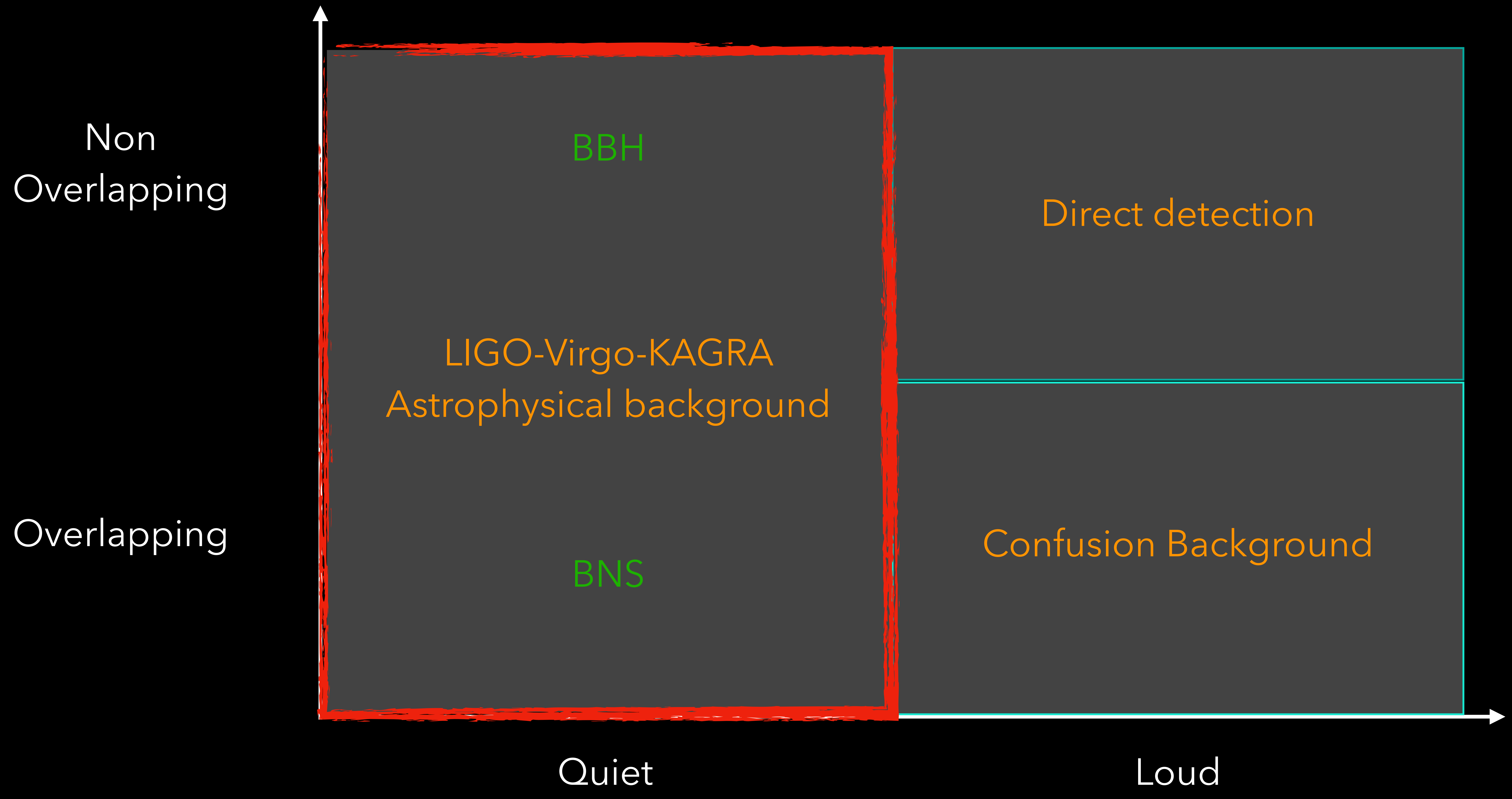

WHAT DETECTION METHODS CAN WE USE?

The GWB signal looks more like noise in a single detector.

What can be done:

- Identify features that distinguish between the expected signal and noise.
  - Measure our detector's noise sources well enough in amplitude and spectral shape.
- Detectors with uncorrelated noise: cross-correlation separates the signal from the noise.

WHAT DETECTION METHODS CAN WE USE?

The GWB signal looks more like noise in a single detector.

What can be done:

- Identify features that distinguish between the expected signal and noise.
  - Measure our detector's noise sources well enough in amplitude and spectral shape.
- Detectors with uncorrelated noise: cross-correlation separates the signal from the noise.

Data from two detectors: $d_1 = h + n_1 \qquad d_2 = h + n_2$ $\quad h$ −> common GW signal component

Expected value of cross-correlation: $\langle d_1 d_2 \rangle = \langle h^2 \rangle + \langle n_1 n_2 \rangle + \langle h n_2 \rangle + \langle n_1 h \rangle = \langle h^2 \rangle + \langle n_1 n_2 \rangle$ (with $\langle h n_2 \rangle \to 0$, $\langle n_1 h \rangle \to 0$)

Assuming detector noise is uncorrelated*: $\langle d_1 d_2 \rangle = \langle h^2 \rangle + \langle n_1 n_2 \rangle$ (with $\langle n_1 n_2 \rangle \to 0$)

$$\langle d_1 d_2 \rangle = \langle h^2 \rangle \equiv S_h$$

Cross-correlation separates the signal from the noise

S_h → Intensity of the background

WHAT DETECTION METHODS CAN WE USE?

Allen, Romano: PRD 59:102001,1999
Romano, Cornish: LRR (2017) 20:2

Cross correlation estimator:

$$\hat{C}^{IJ}(f) \propto \frac{2}{T} \frac{\Re[\tilde{s}_I^*(f)\, \tilde{s}_J(f)]}{\Gamma_{IJ}(f)\, S_0(f)}$$

Variance:

$$\sigma_{IJ}^2(f) \approx \frac{1}{2T\,\Delta f} \frac{P_I(f)\, P_J(f)}{\Gamma_{IJ}^2(f)\, S_0^2(f)}$$

Signal to noise ratio:

$$\mathrm{SNR} = \frac{3H_0^2\sqrt{T}}{10\pi^2} \left(\int_{-\infty}^{\infty} \mathrm{d}f \, \frac{\Omega_{\mathrm{GW}}^2(|f|)\, \Gamma_{12}^2(|f|)}{|f|^6\, P_1(|f|)\, P_2(|f|)} \right)^{1/2}$$

O3 ISOTROPIC RESULTS

PRD104, 022004 (2021)

The observed cross-correlation spectra combining data from all three observing runs of LIGO-Virgo-KAGRA detectors: The spectrum is consistent with expectations from uncorrelated, Gaussian noise.

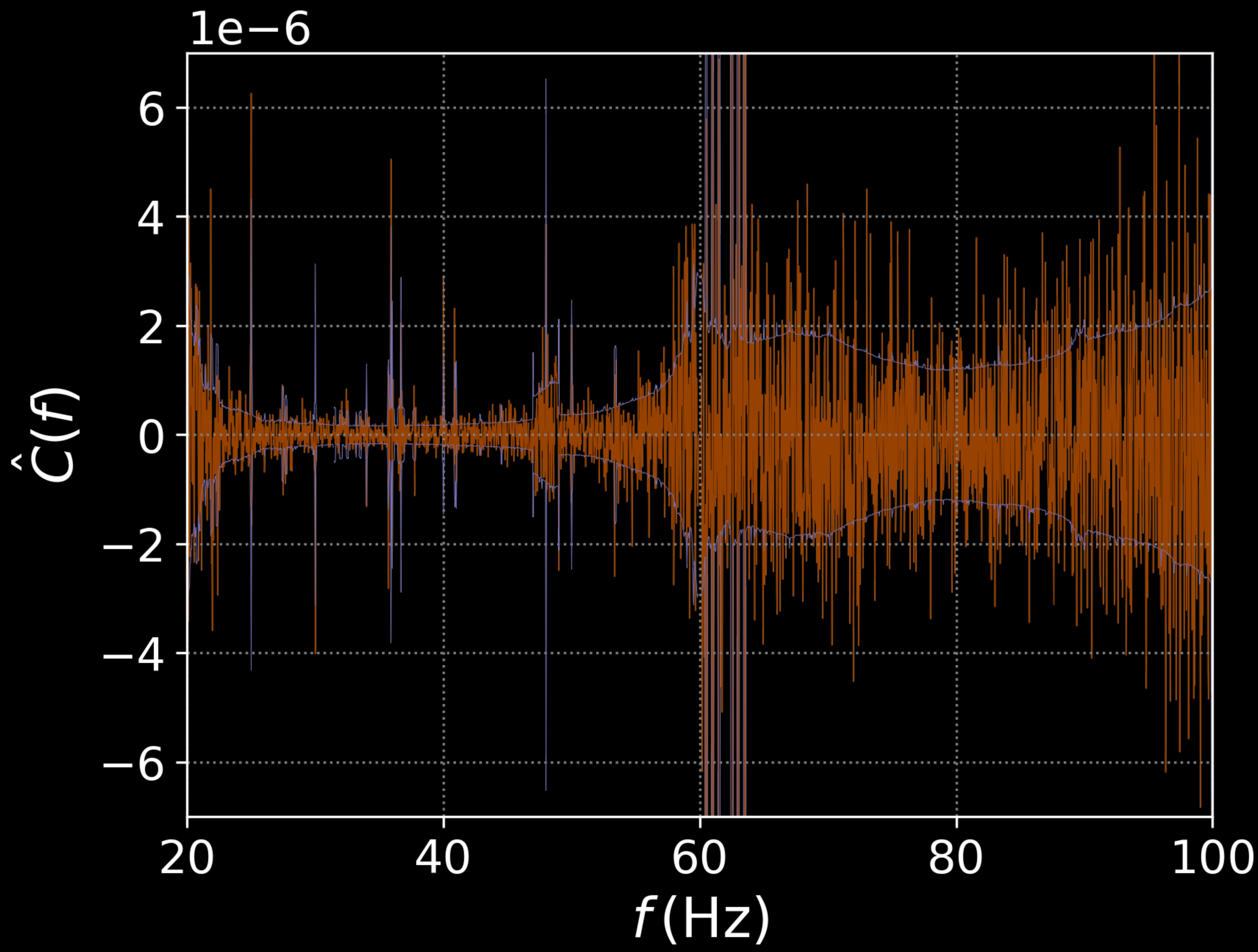

SENSITIVITY PROJECTION

LVK PRD104, 022004 (2021)
LVK PRX:13, 011048 (2023)

$$\Omega_{\rm CBC}(f) \propto \int_0^\infty dz\, R(z)\, \frac{1}{(1+z)E(z)}\, f_s \left(\frac{dE_{\rm gw}}{df_s}\right)$$

$\Omega_{\rm GW}(25{\rm Hz}) = 6.9 \times 10^{-10}$

Results from third observing run of LIGO-Virgo-KAGRA collaboration.

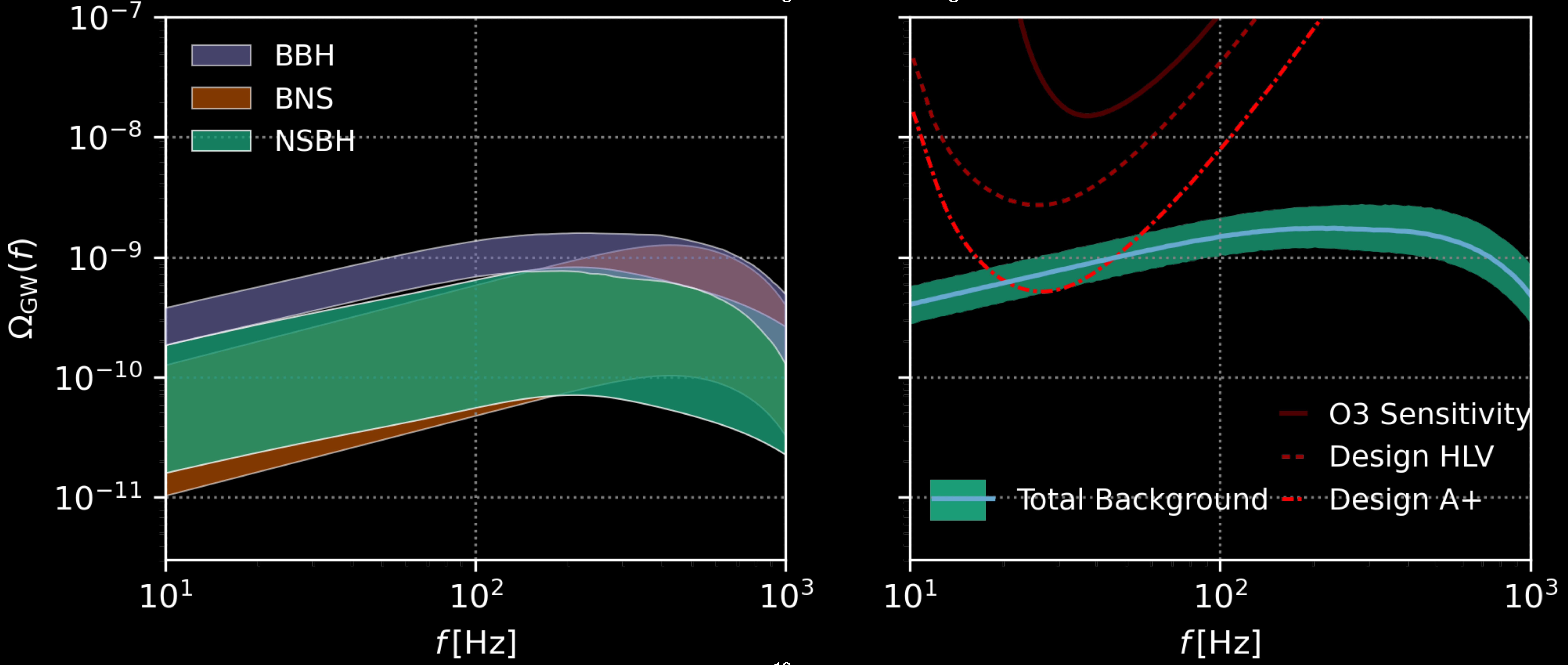

WE ARE NOW AT:

— **1965: Penzias & Wilson**

A MEASUREMENT OF EXCESS ANTENNA TEMPERATURE
AT 4080 Mc/s

Measurements of the effective zenith noise temperature of the 20-foot horn-reflector antenna (Crawford, Hogg, and Hunt 1961) at the Crawford Hill Laboratory, Holmdel, New Jersey, at 4080 Mc/s have yielded a value about 3.5° K higher than expected. This excess temperature is, within the limits of our observations, isotropic, unpolarized, and free from seasonal variations (July, 1964–April, 1965). A possible explanation for the observed excess noise temperature is the one given by Dicke, Peebles, Roll, and Wilkinson (1965) in a companion letter in this issue.

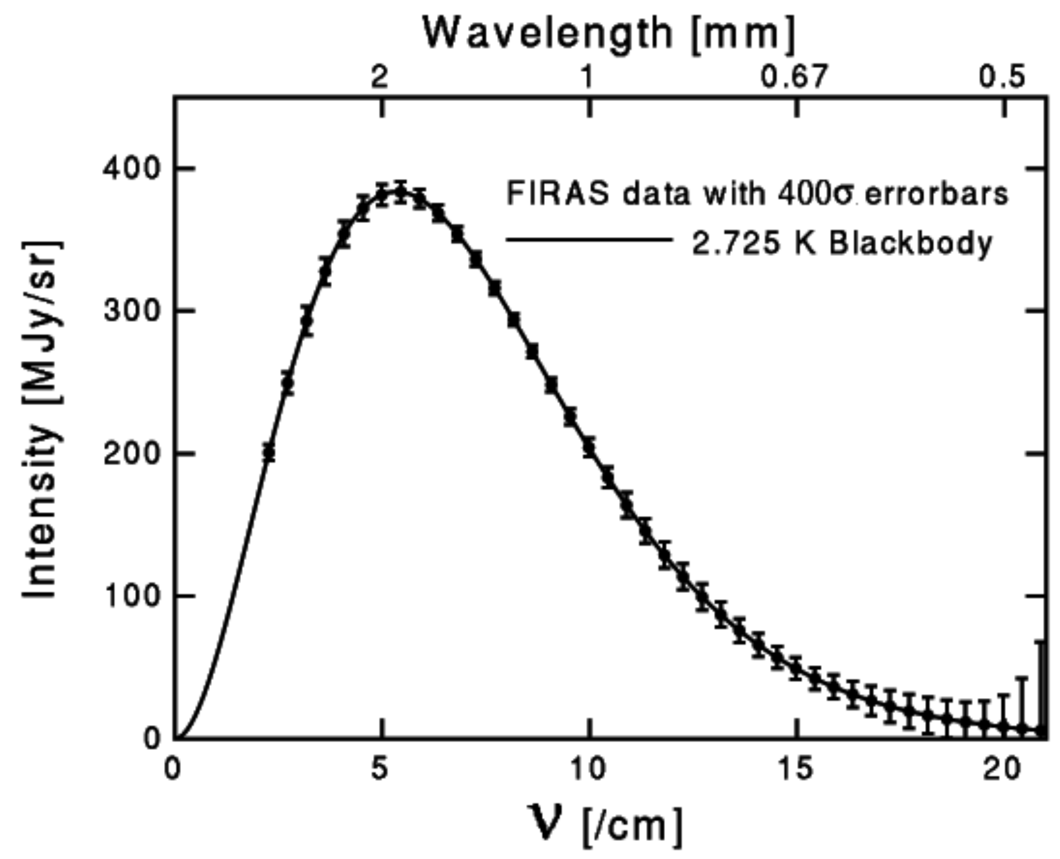

2.725 K blackbody

— **1992: COBE**

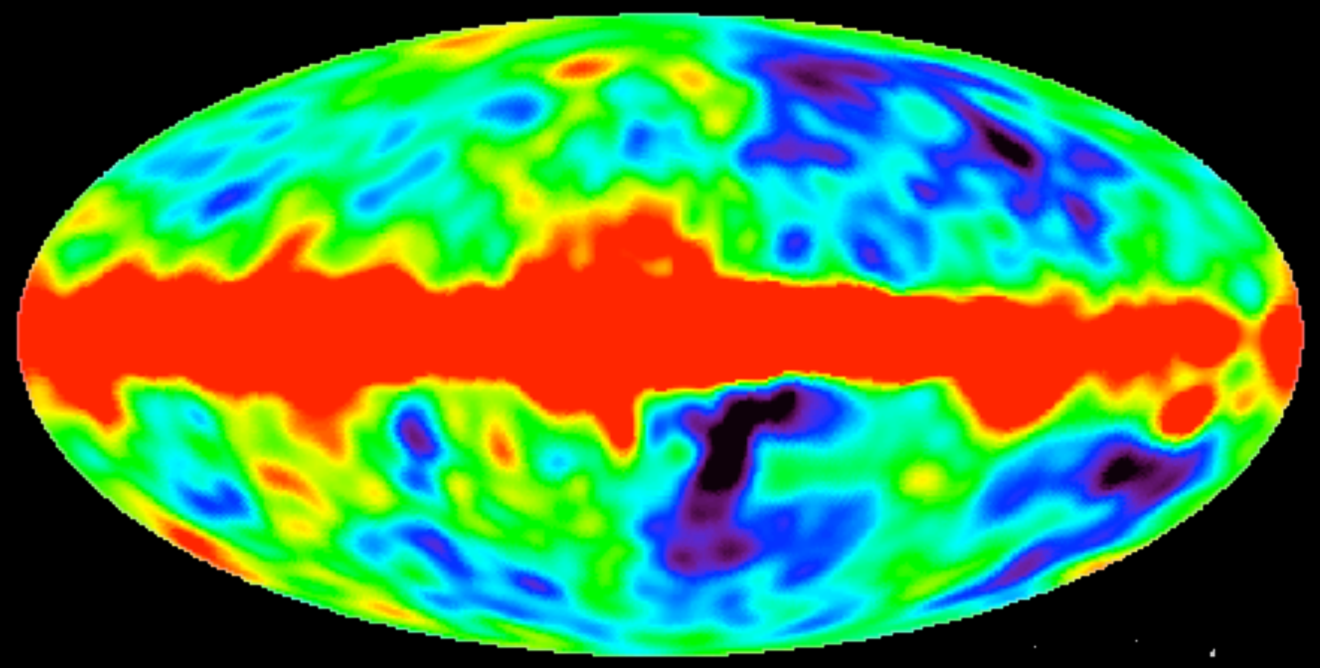

— **2013: WMAP, Planck**

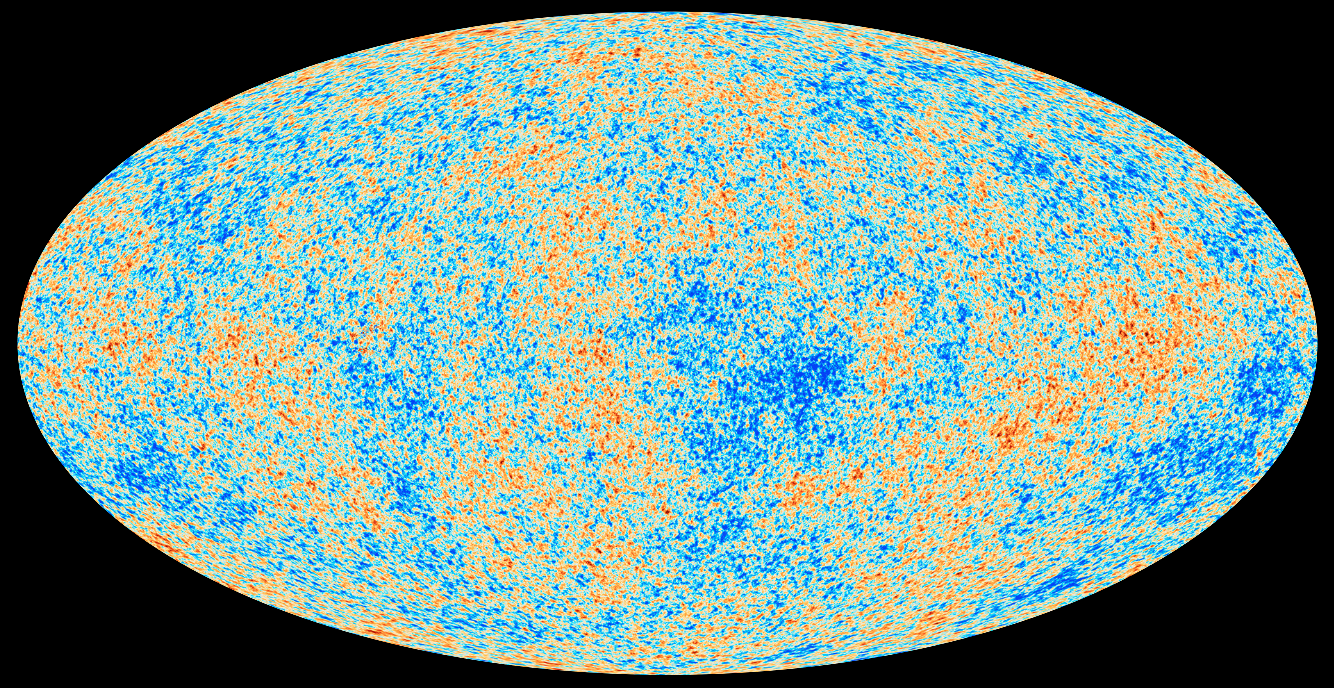

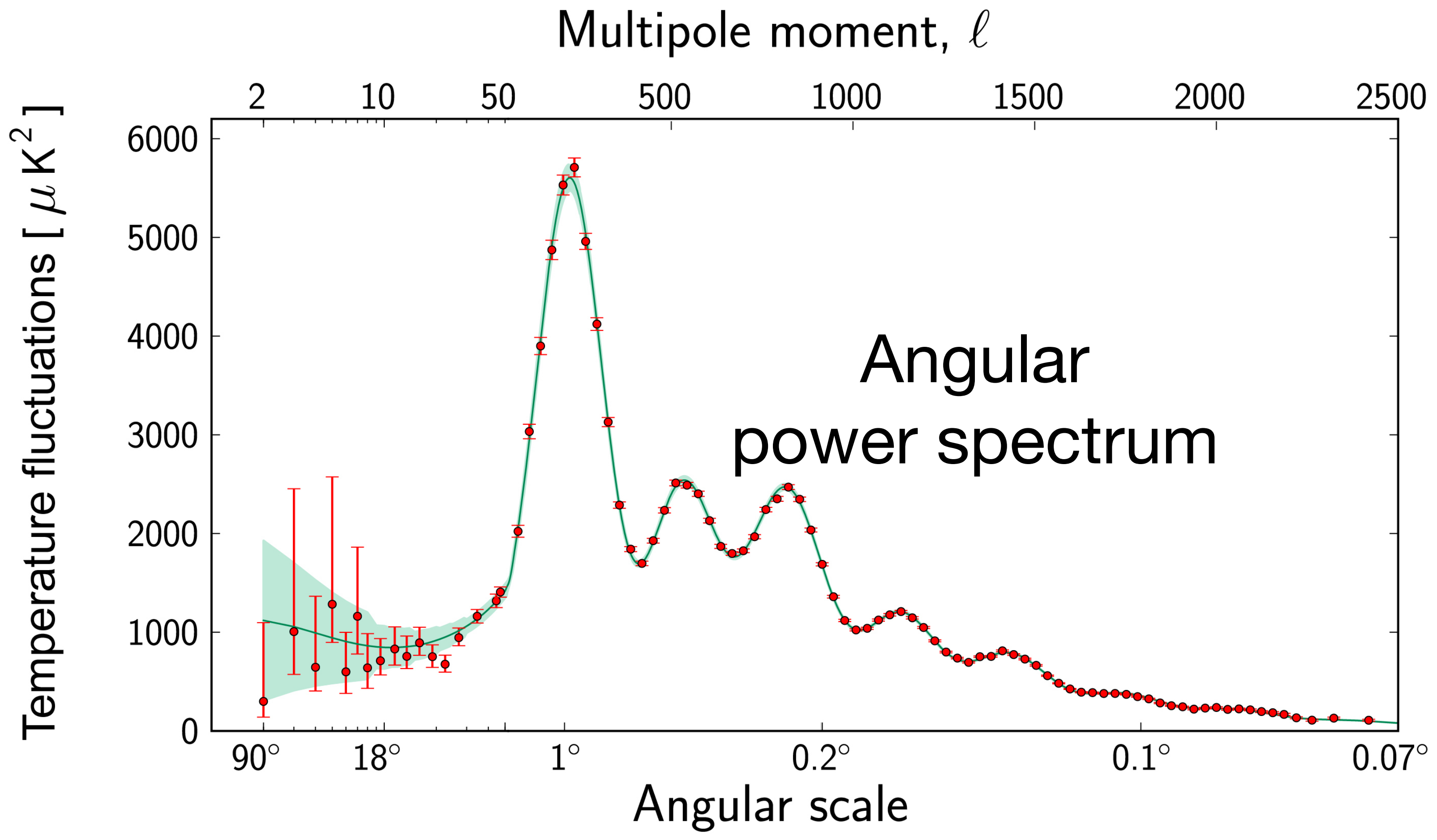

— **2025:** **We are yet to detect the isotropic component of the GWB!**

WE ARE NOW AT:

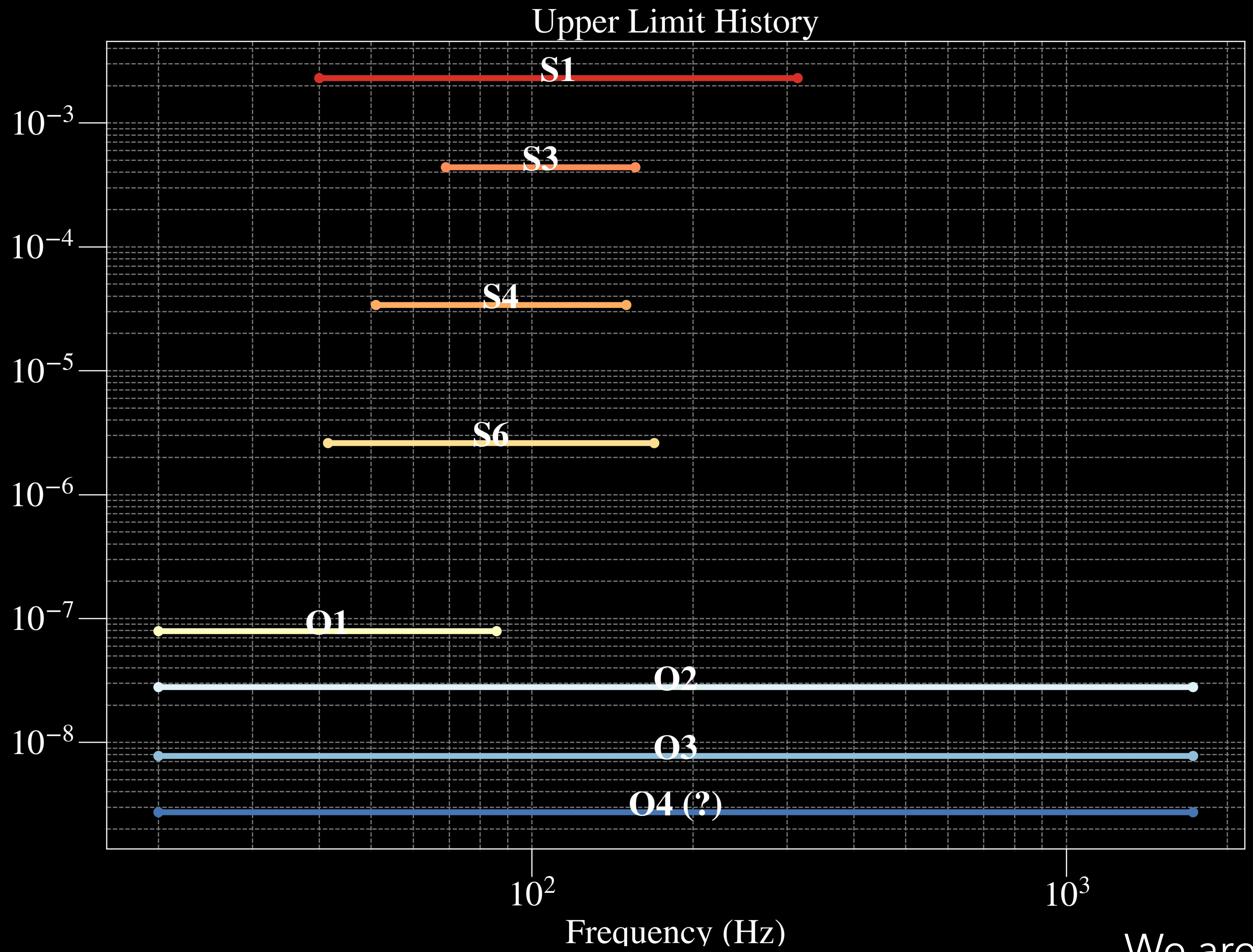

We are reaching there…

ISOTROPIC GWB

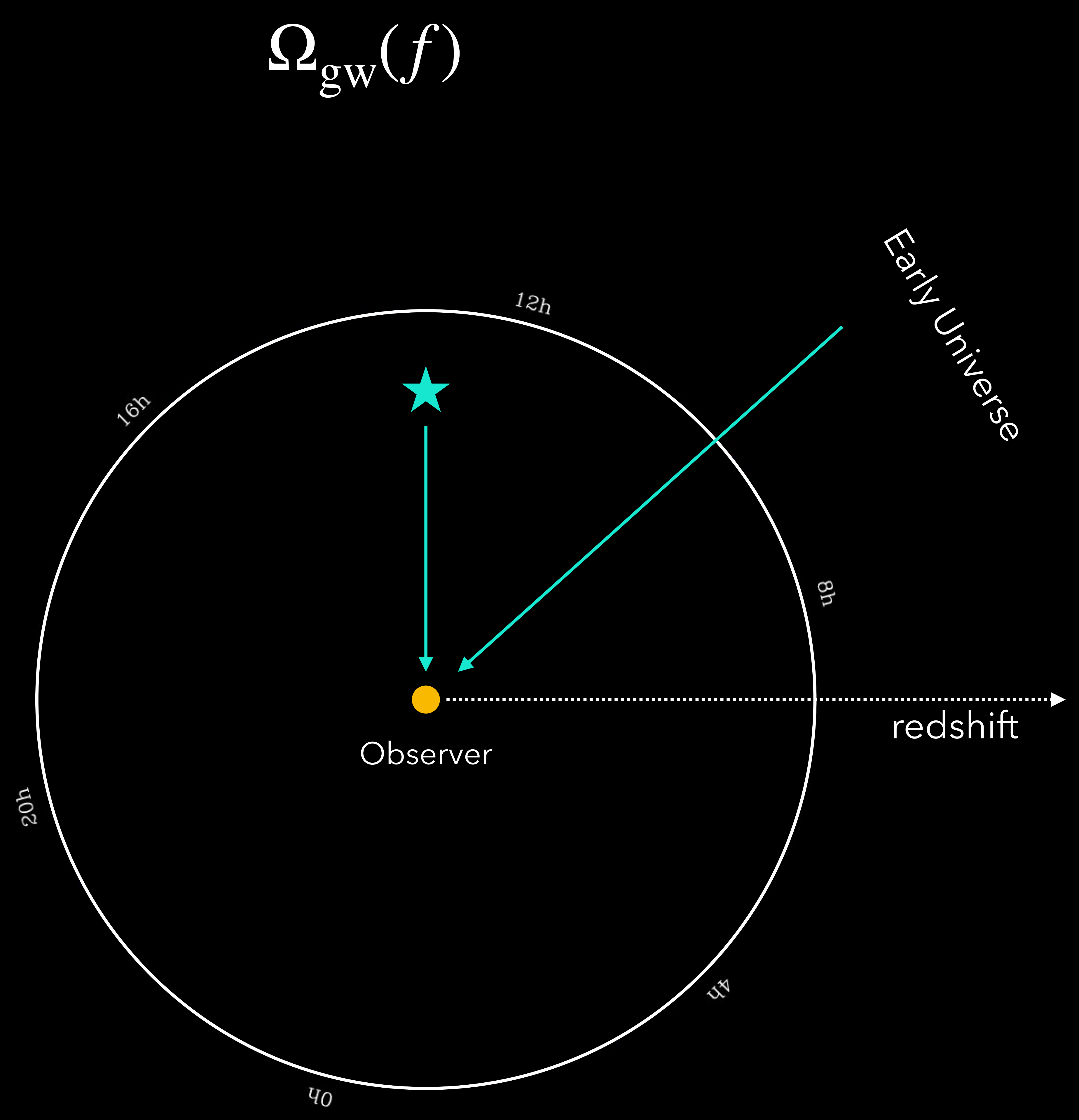

- sources isotropically distributed
- propagation along straight line
- no anisotropy in received flux

Slide adapted from G. Cusin's talk

ANISOTROPIC GWB

- Anisotropic distribution of the emitting sources.
- Due to propagation: as gravitational-wave propagate, they accumulate line-of-sight effects, crossing different matter density fields which are inhomogeneously distributed in the Universe.

$$\Omega_{\rm gw}(f, \hat{n})$$

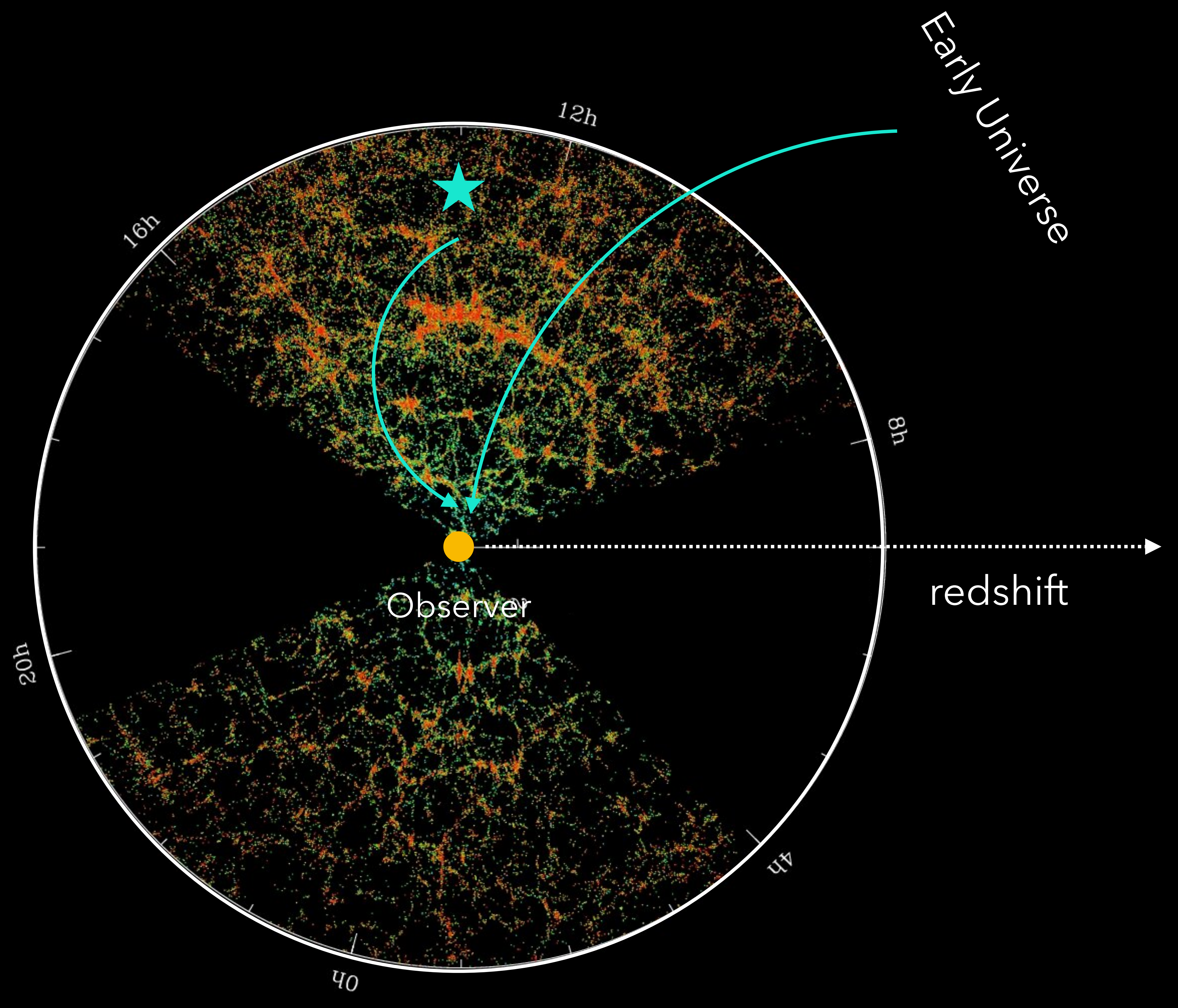

Slide adapted from G. Cusin's talk

ANISOTROPIC GWB

$$\Omega_{\mathrm{gw}}(f) \longrightarrow \Omega_{\mathrm{gw}}(f, \hat{n})$$

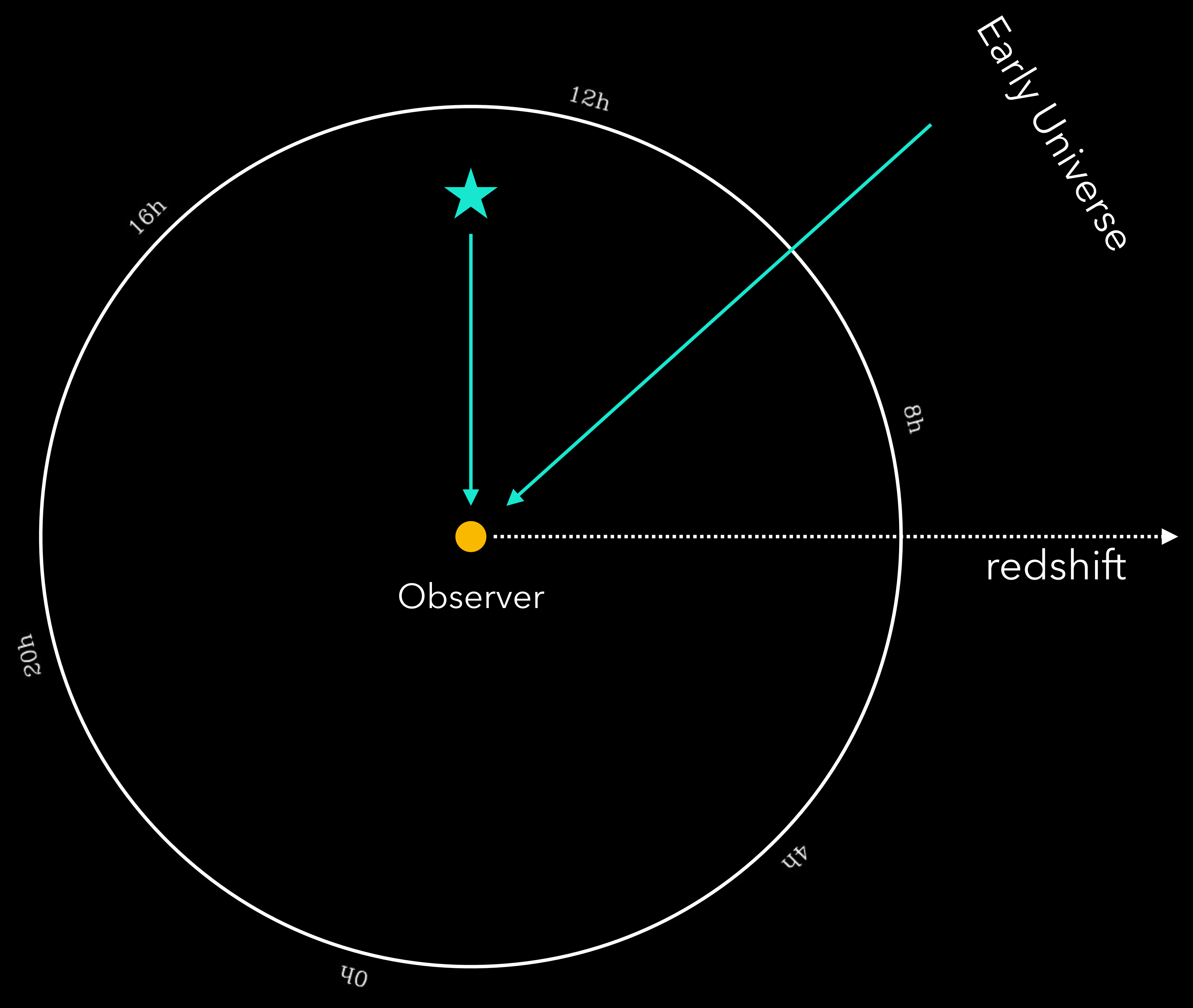

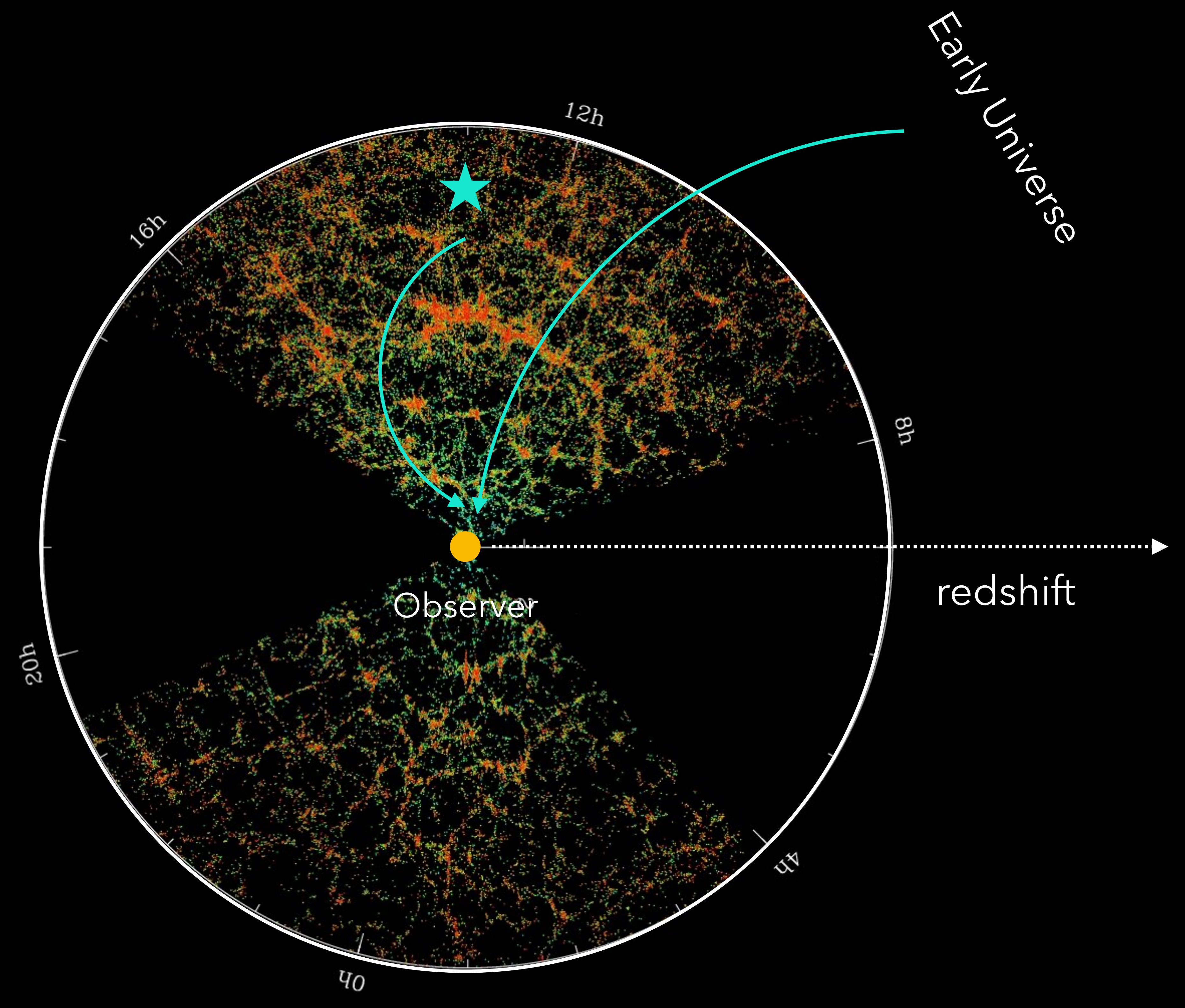

Slide adapted from G. Cusin's talk

HOW DO WE MAP THE GWB SKY?

http://mwmw.gsfc.nasa.gov/mmw_allsky.html

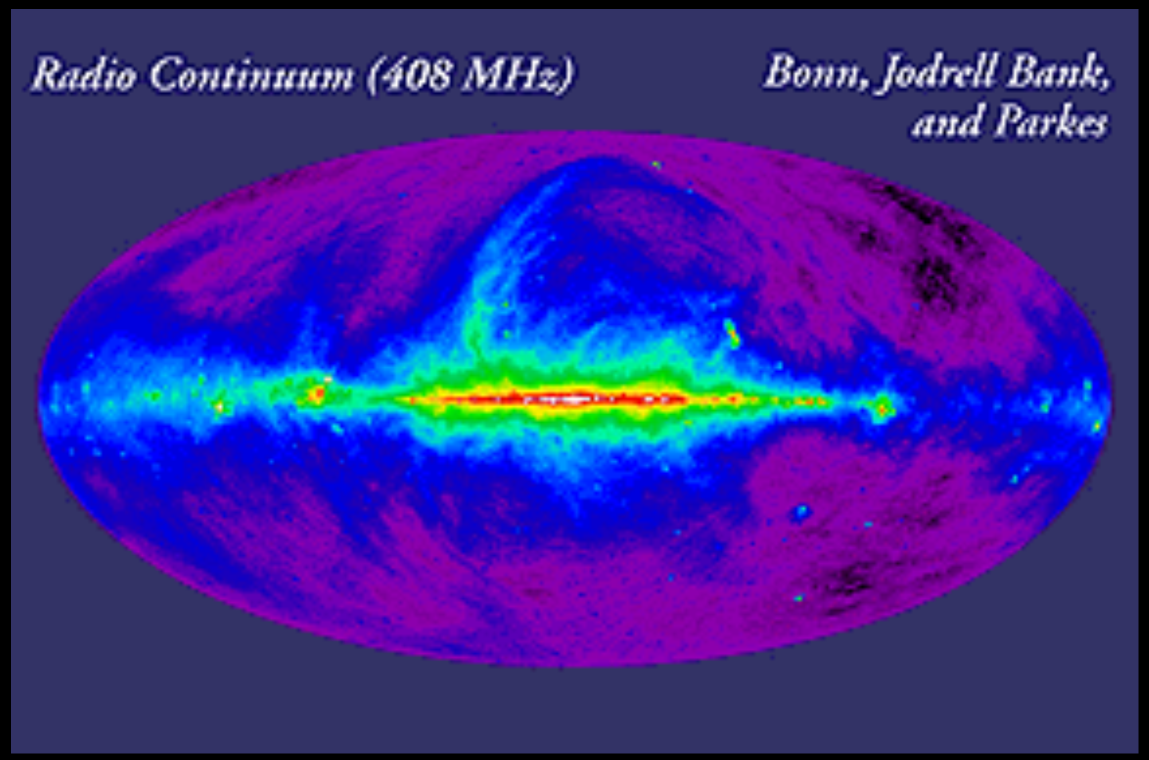

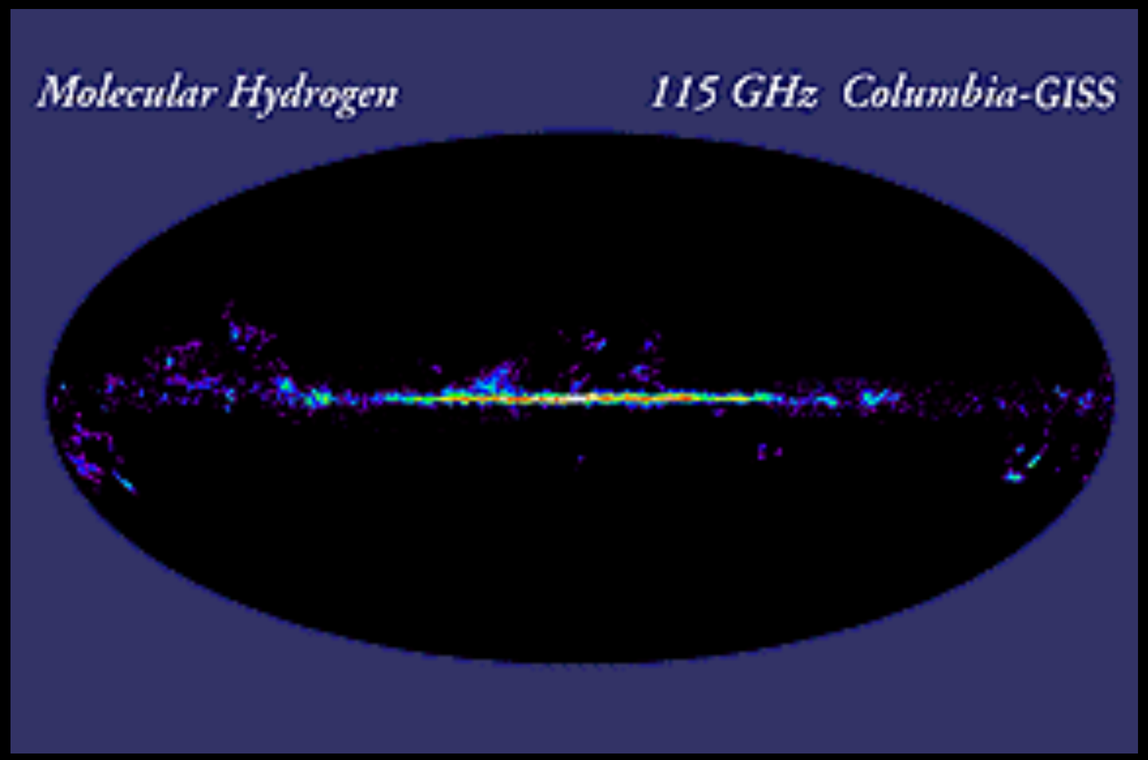

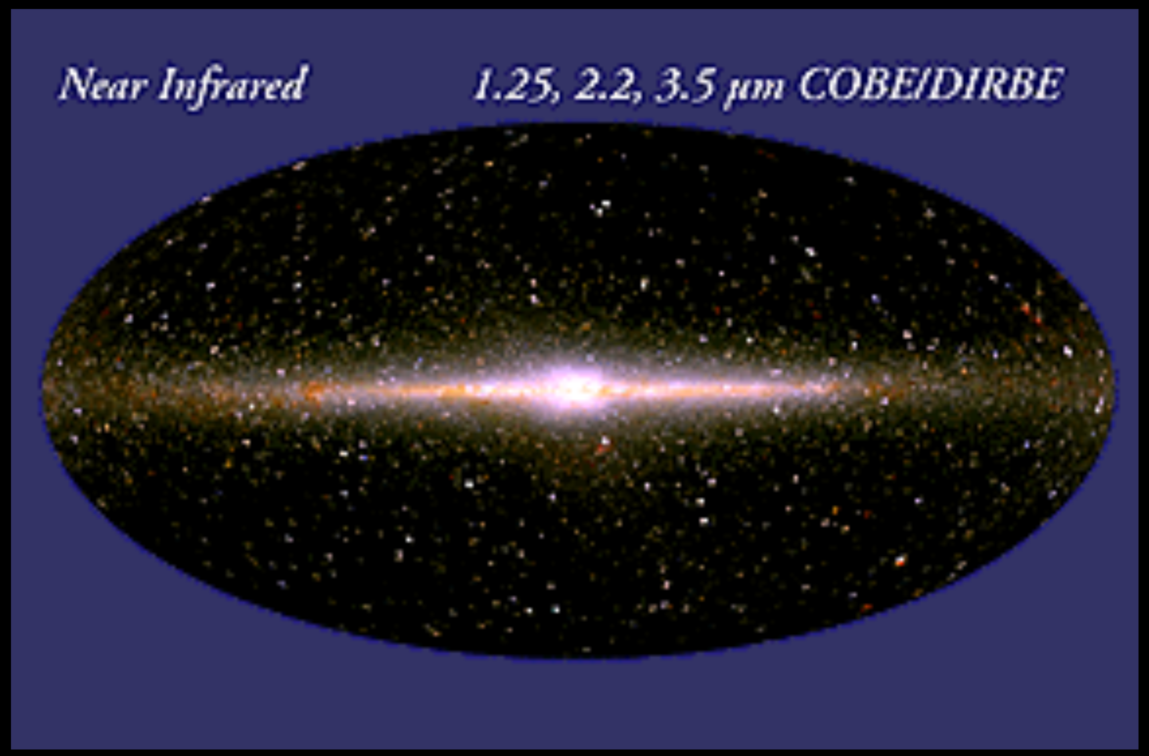

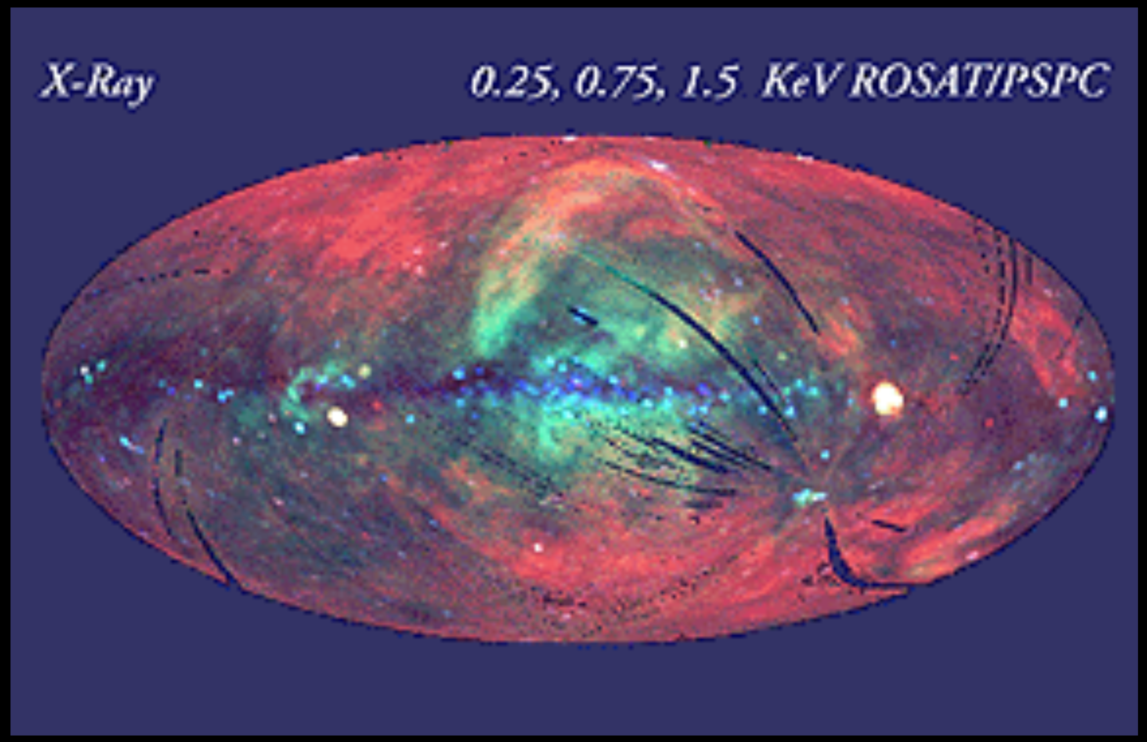

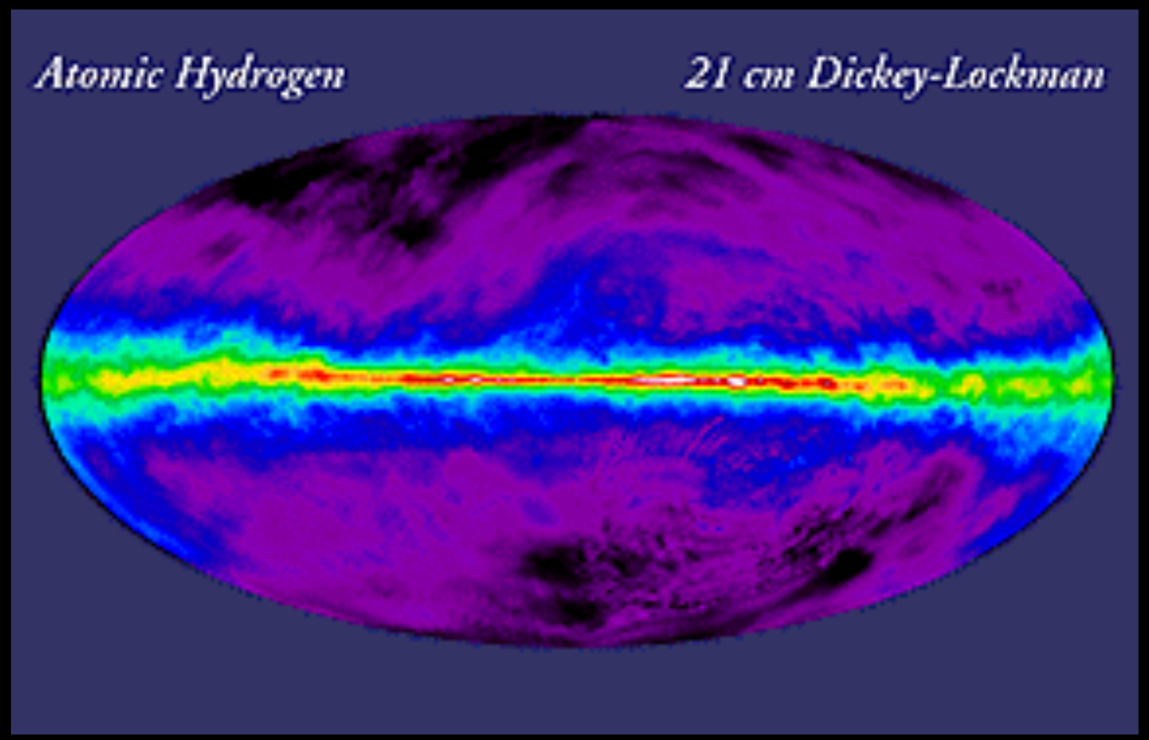

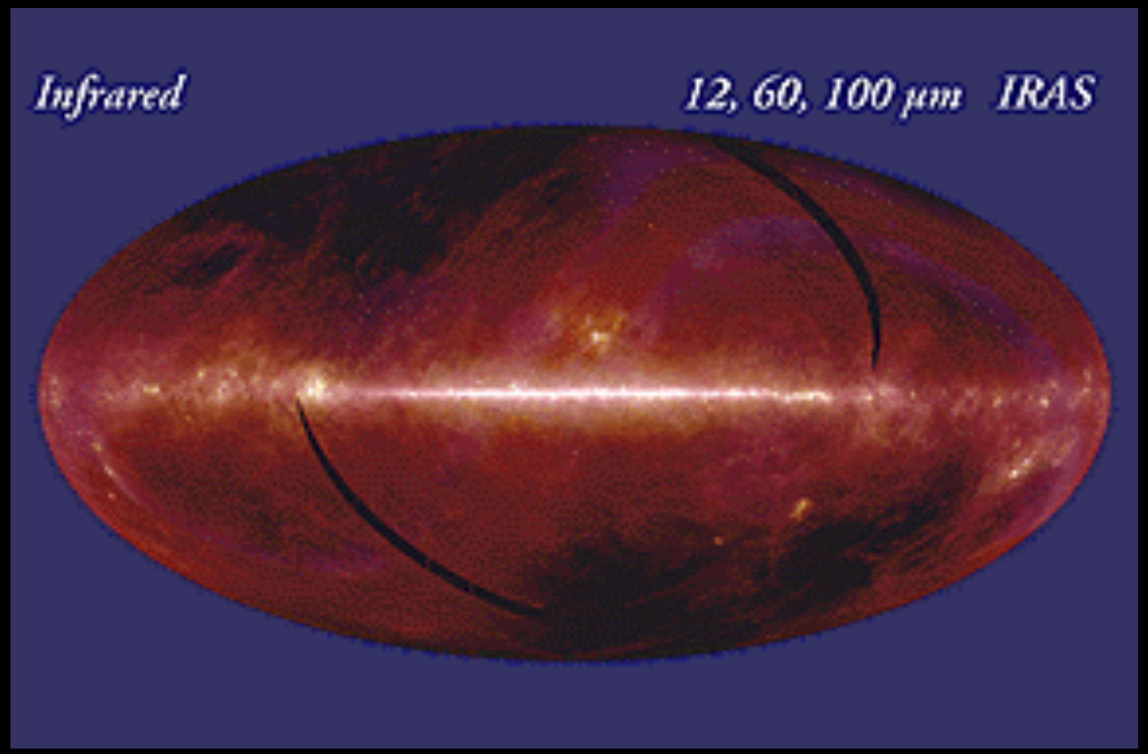

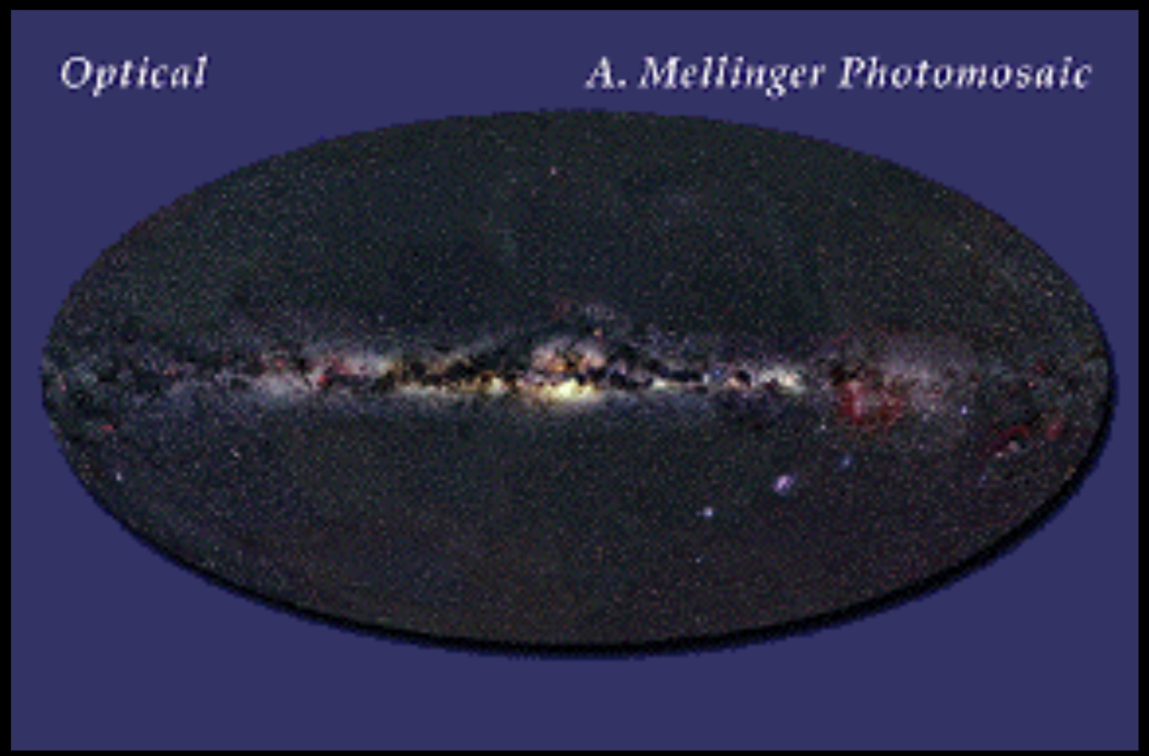

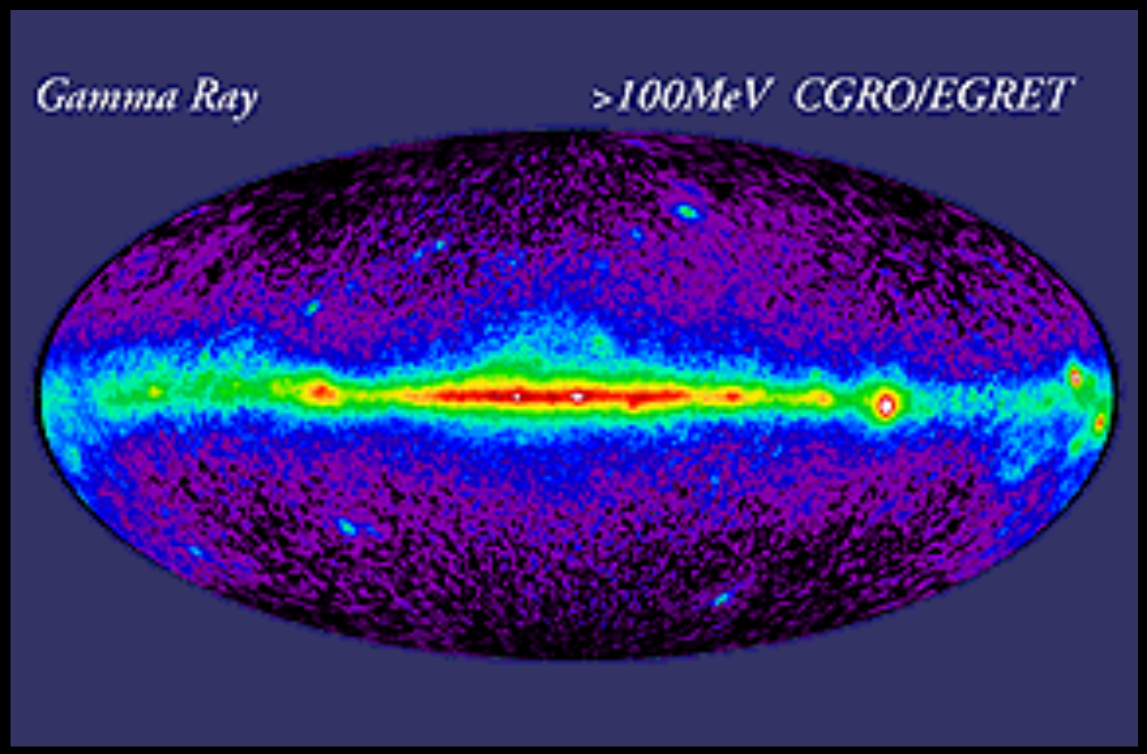

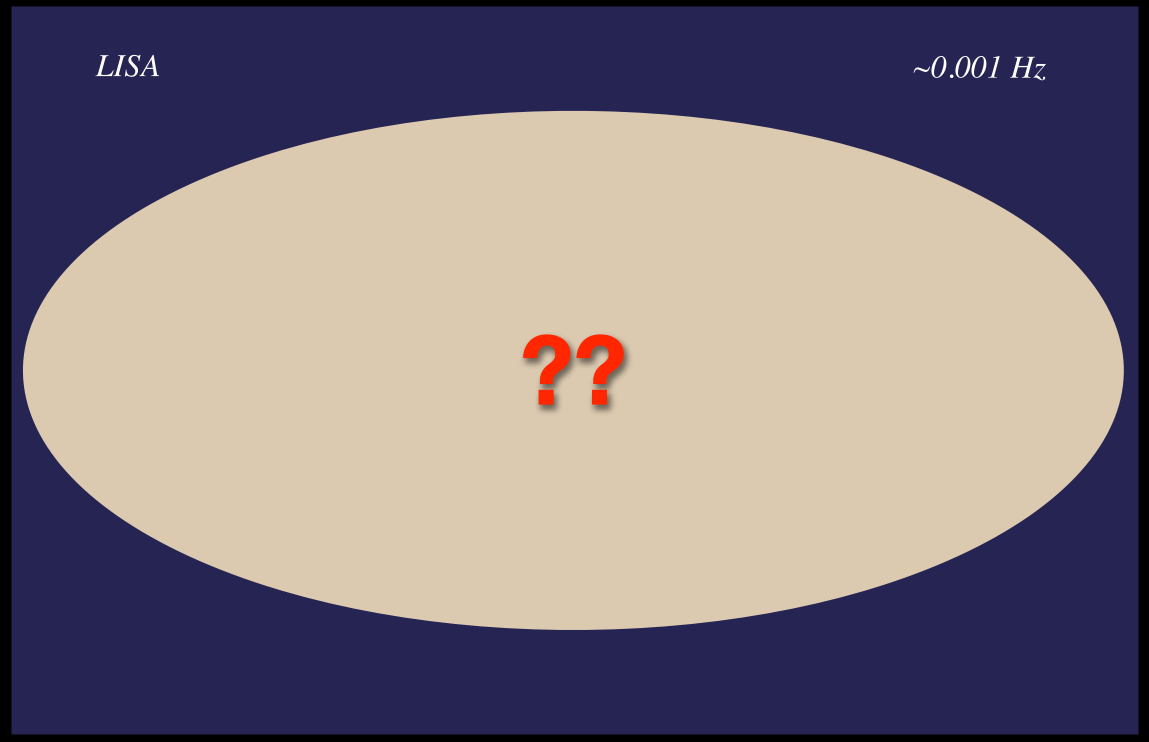

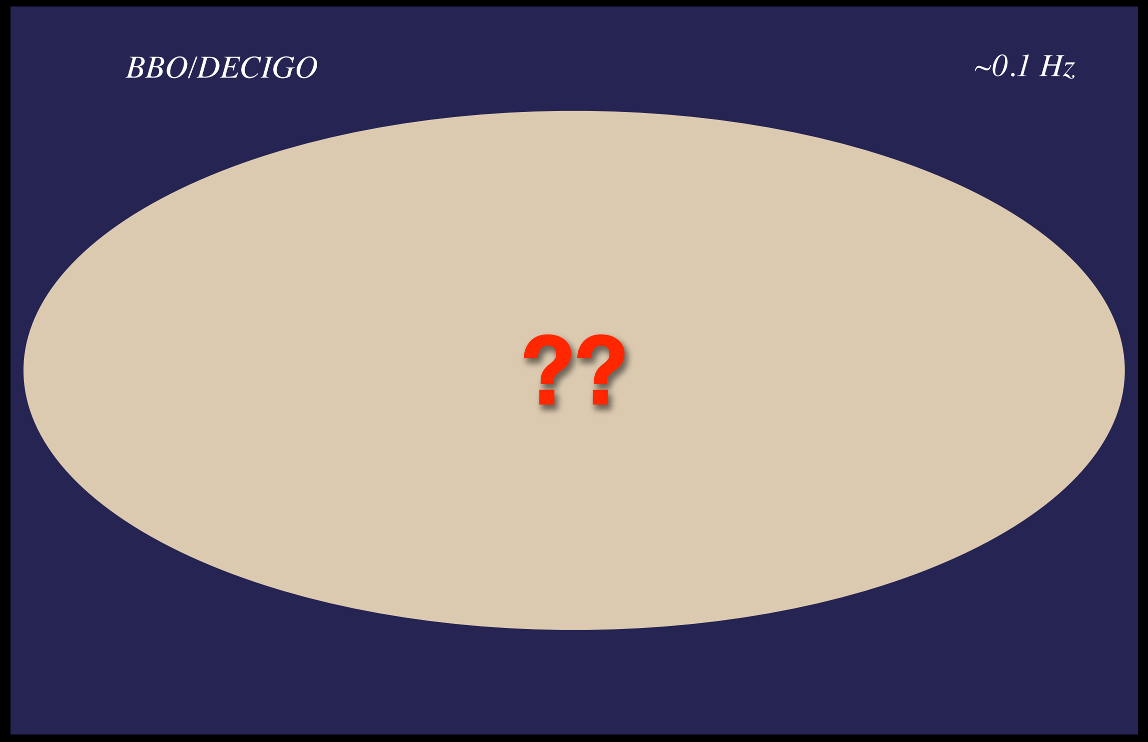

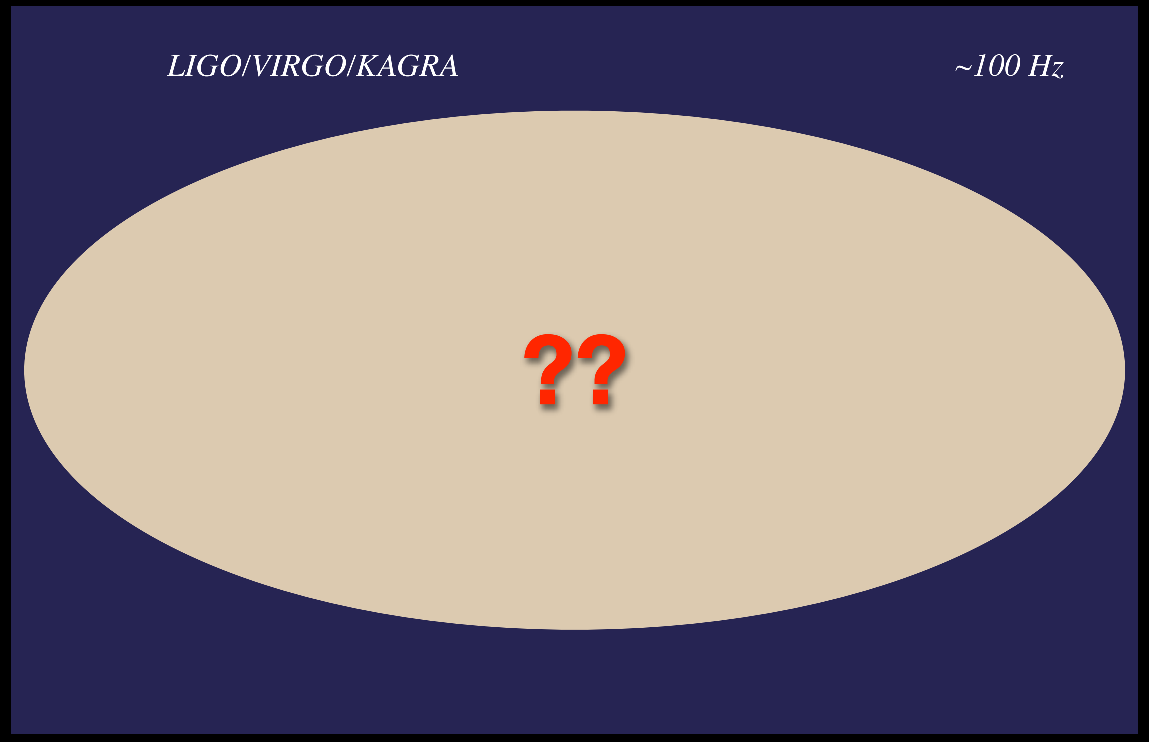

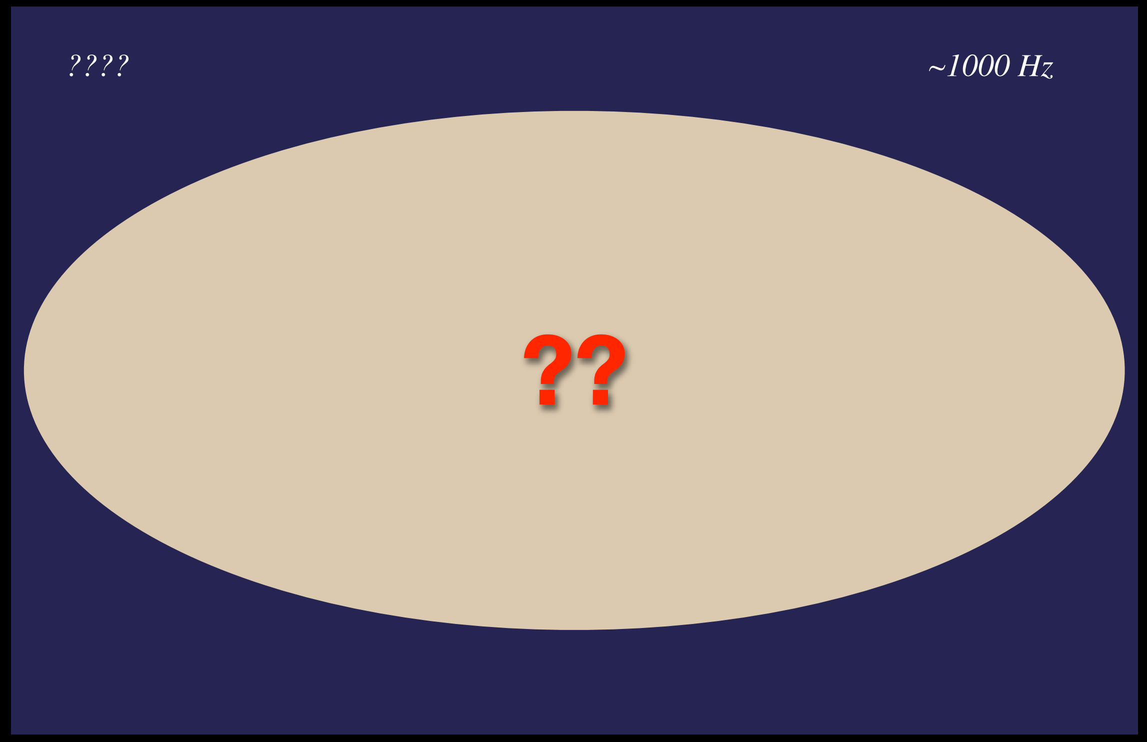

HOW DO WE MAP THE GWB SKY?

Cross-correlation is essentially a one-dimensional map of the sky

ANISOTROPIC SEARCH

S. Ballmer: CQG 23:S179-S186,2006
S. Mitra+: PRD 77 (2008) 042002

How do we extract the anisotropic GWB signal?
How to solve for its directionality?
How do we effectively map this signal on the sky?

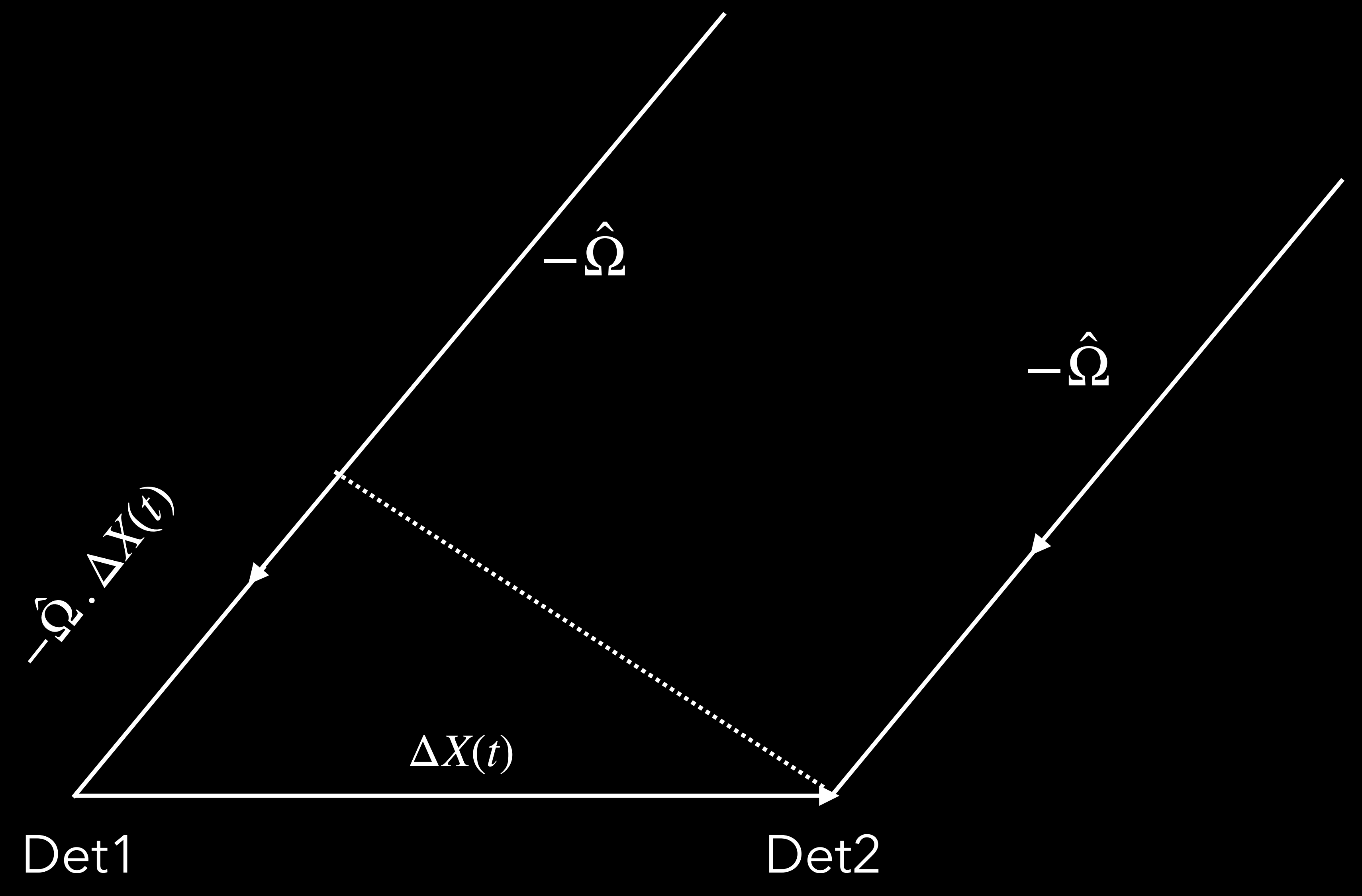

- The time delay between two detectors
- Rotation of the earth.

GWB energy density $\Omega_{\rm gw}(f, \hat{\mathbf{n}}) \equiv \frac{f}{\rho_c}\frac{d\rho_{\rm GW}}{df} = \frac{2\pi^2}{3H_0^2} f^3 \mathscr{P}(f, \hat{\mathbf{n}})$

Cross-correlation is essentially a one-dimensional map of the sky.

Anisotropy can be expanded in pixel or spherical harmonic basis

$$\mathscr{P}(f, \hat{\mathbf{n}}) = \sum_p \mathscr{P}_p(f)\, e_p(\hat{\mathbf{n}})$$

ANISOTROPIC SEARCH

Cross-correlation is essentially a one-dimensional map of the sky.

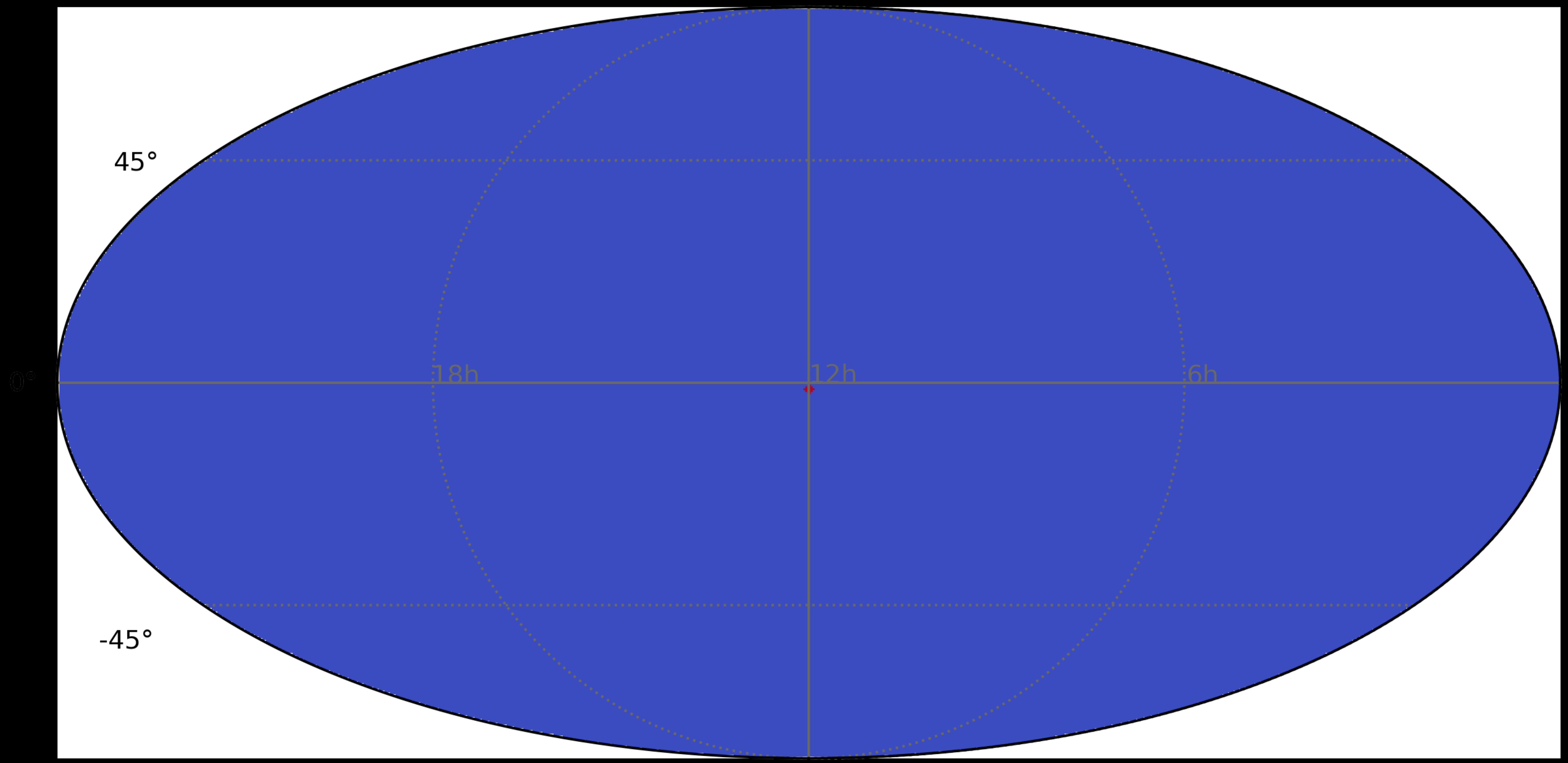

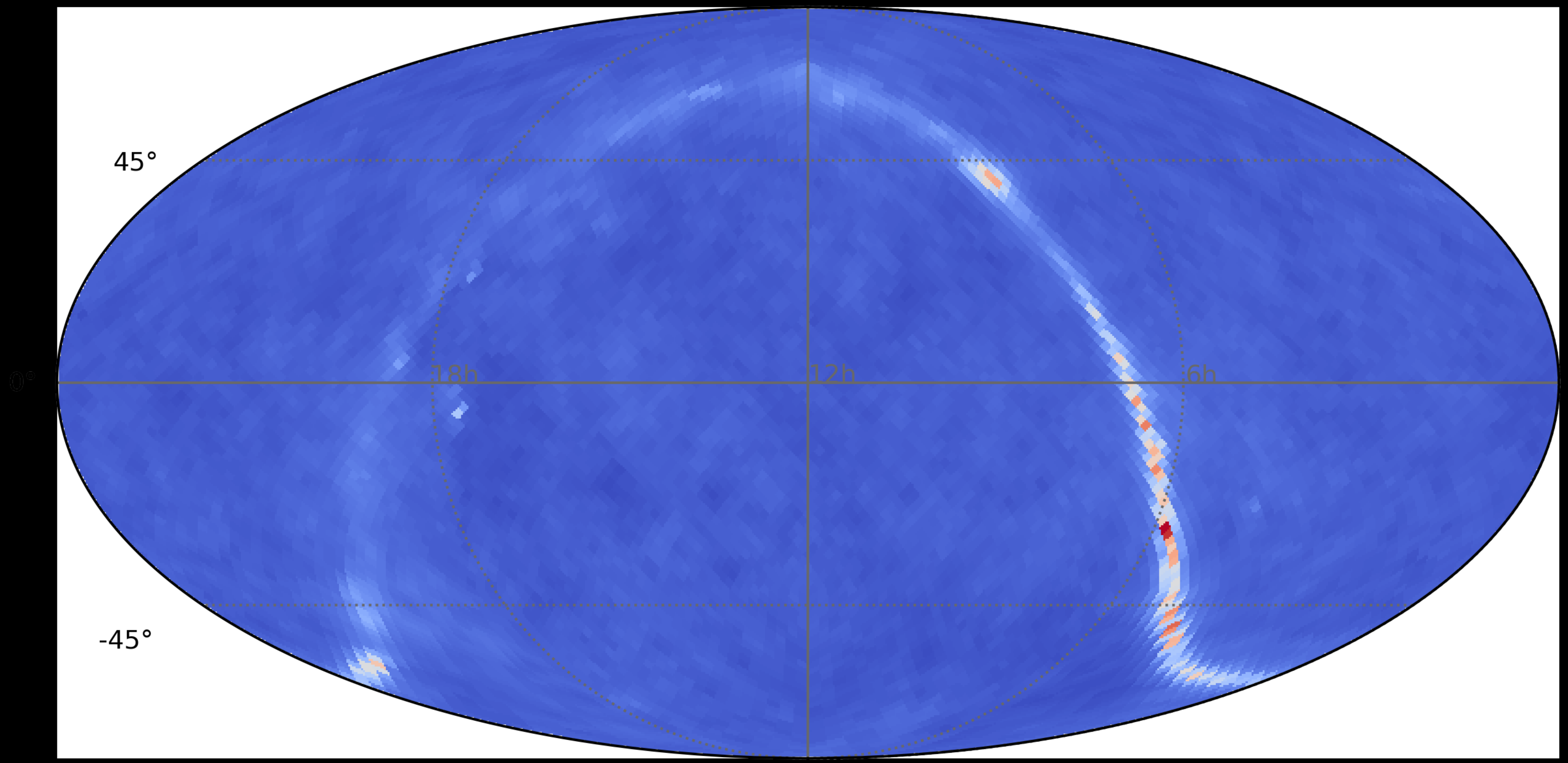

ANISOTROPIC SEARCH

Cross-correlation is essentially a one-dimensional map of the sky.

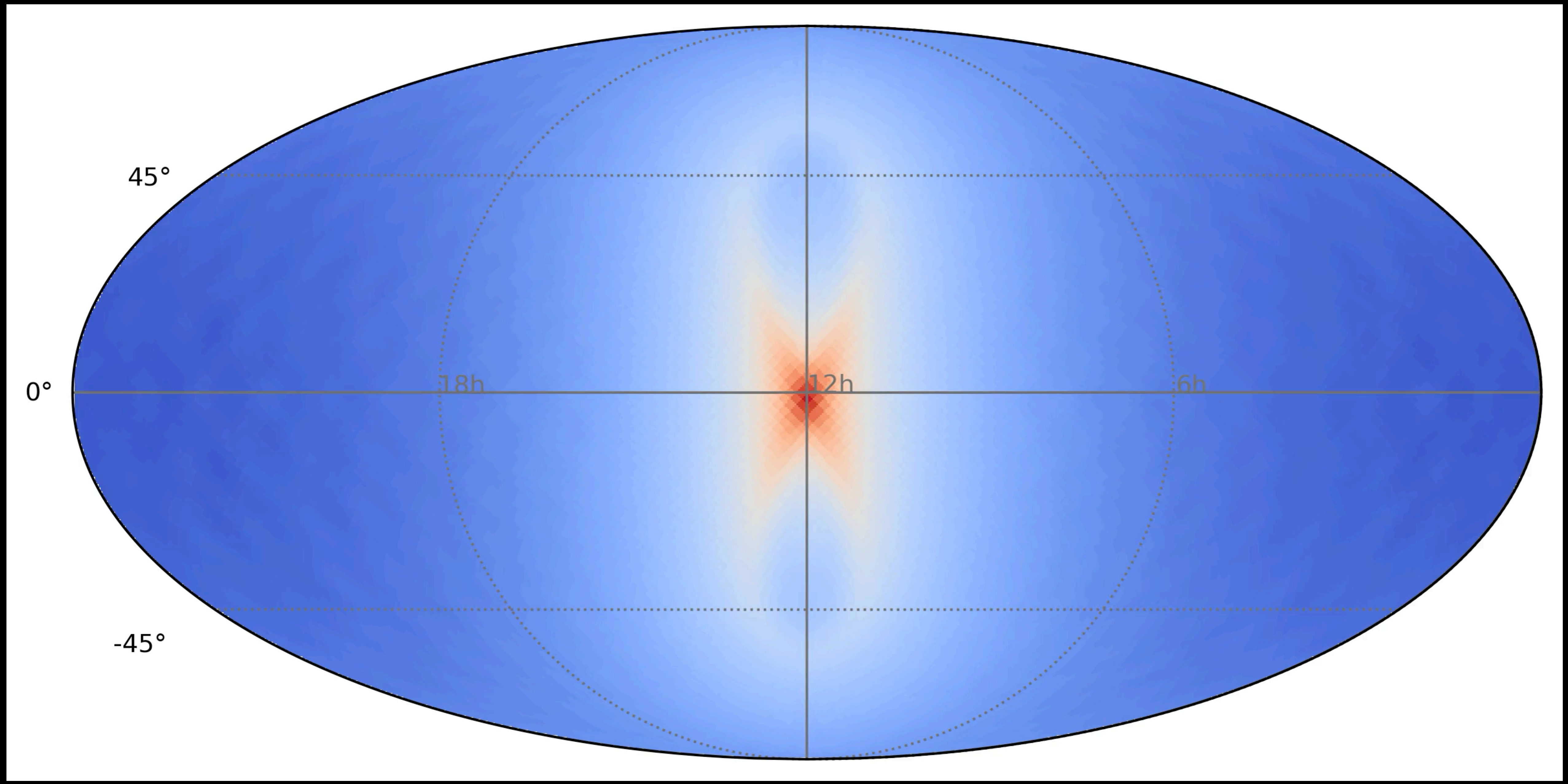

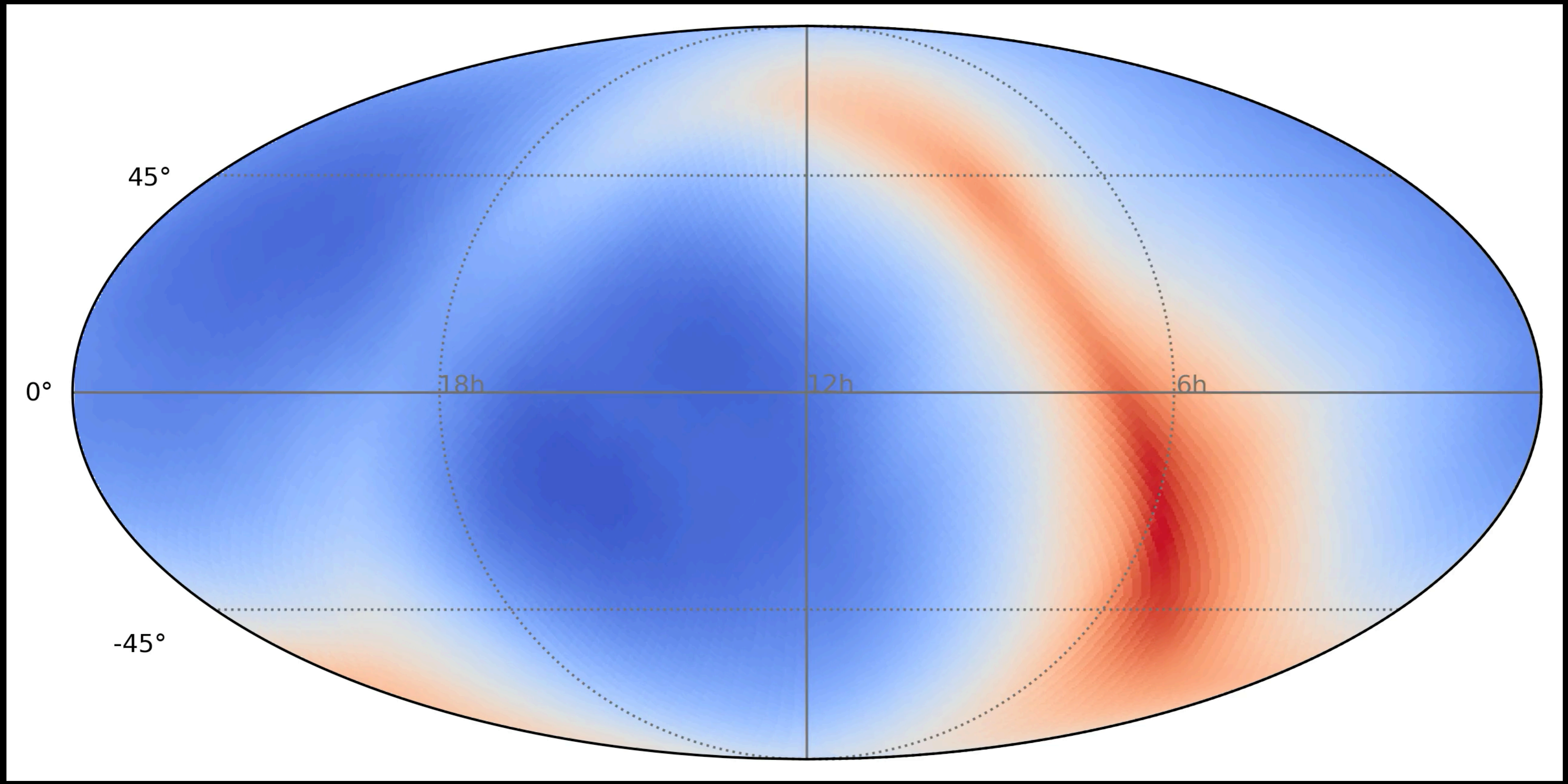

O3 ANISOTROPIC RESULT

PRD 104, 022005 (2021)

- Broadband: point sources with different power-law spectra.
- Narrowband: point sources having narrow GW frequency band (SN 1987A, ScoX-1, GC)
- Spherical harmonics search: Extended or diffuse sources - measure angular power spectra

All-sky BBR Results			Max SNR (% p-value)				Upper limit ranges (10^{-8})	
α	Ω_{GW}	$H(f)$	HL(O3)	HV(O3)	LV(O3)	O1 + O2 + O3 (HLV)	O1 + O2 + O3 (HLV)	O1 + O2 (HL)
0	Constant	$\propto f^{-3}$	2.3 (66)	3.4 (24)	3.1 (51)	2.6 (23)	1.7–7.6	4.4–21
$2/3$	$\propto f^{2/3}$	$\propto f^{-7/3}$	2.5 (59)	3.7 (14)	3.1 (62)	2.7 (24)	0.85–4.1	2.3–12
3	$\propto f^3$	Constant	3.7 (32)	3.6 (47)	4.1 (12)	3.6 (20)	0.013–0.11	0.046–0.32

O3 ANISOTROPIC RESULT

PRD 104, 022005 (2021)

- Broadband: point sources with different power-law spectra.
- Narrowband: point sources having narrow GW frequency band (SN 1987A, ScoX-1, GC)
- Spherical harmonics search: Extended or diffuse sources - measure angular power spectra

Narrow band Radiometer Results					
Direction	**Max SNR**	p**-value (%)**	**Frequency (Hz) (± 0.016 Hz)**	**Best upper limit (10^{-25})**	**Frequency band (Hz)**
Scorpius X-1	4.1	65.7	630.31	2.1	189.31–190.31
SN 1987A	4.9	1.8	414.0	1.7	185.13–186.13
Galactic Center	4.1	62.3	927.25	2.1	202.56–203.56

O3 ANISOTROPIC RESULT

PRD 104, 022005 (2021)

- Broadband: point sources with different power-law spectra.
- Narrowband: point sources having narrow GW frequency band (SN 1987A, ScoX-1, GC)
- Spherical harmonics search: Extended or diffuse sources - measure angular power spectra

SHD Results

			Max SNR (% p-value)				Upper limit range (10^{-9})	
α	Ω_{GW}	$H(f)$	HL(O3)	HV(O3)	LV(O3)	O1 + O2 + O3 (HLV)	O1 + O2 + O3 (HLV)	O1 + O2 (HL)
0	Constant	$\propto f^{-3}$	1.6 (78)	2.1 (40)	1.5 (83)	2.2 (43)	3.2–9.3	7.8–29
$2/3$	$\propto f^{2/3}$	$\propto f^{-7/3}$	3.0 (13)	3.9 (0.98)	1.9 (82)	2.9 (18)	2.4–9.3	6.4–25
3	$\propto f^{3}$	Constant	3.9 (12)	4.0 (10)	3.9 (11)	3.2 (60)	0.57–3.4	1.9–11

PyStoch: MAP-MAKING PIPELINE

Ain, Suresh, Mitra PRD 98, 024001 (2018)
Suresh, Ain, Mitra PRD 103, 083024 (2021)

PyStoch : fast HEALPix based GWB mapmaking

↓

perform the whole analysis on a laptop in a few minutes

↓

Produces the narrowband maps as an intermediate result

so separate search for different frequency spectra becomes redundant

* We have used sidereally folded data (PRD 92, 022003 2015) set for this analysis

https://git.ligo.org/stochastic-public/stochastic.git

ALL-SKY ALL-FREQUENCY SEARCH

Phys.Rev.D 105 (2022) 10, 102001

Now we have all the ingredients to perform an all-sky, all-frequency search, which assumes **no** specific power-law model for the GWB

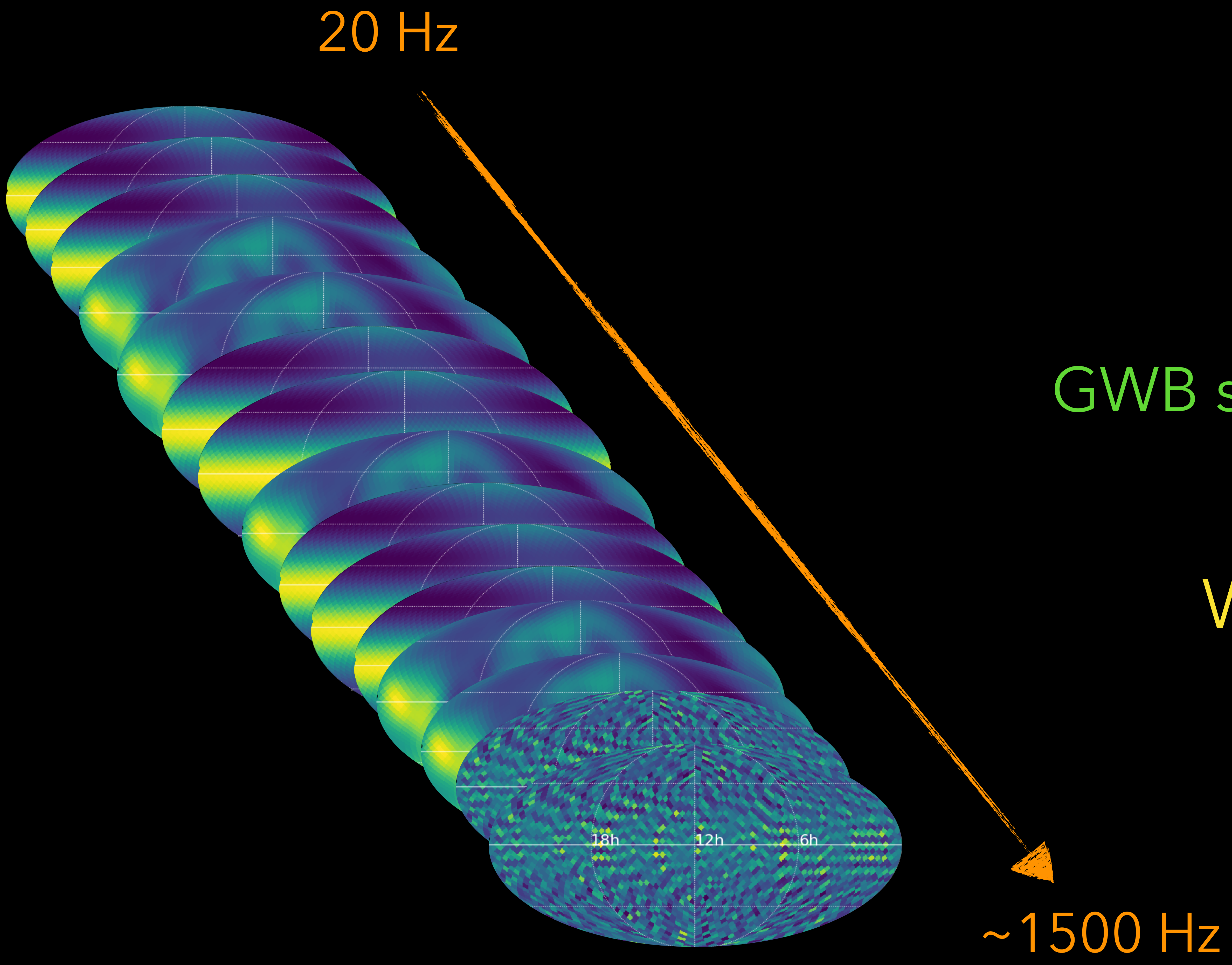

GWB sky maps at every frequency bins

We presented the **first atlas** of GWB sky

Phys.Rev.D 105 (2022) 10, 102001

ALL-SKY ALL-FREQUENCY SEARCH

Phys.Rev.D 105 (2022) 10, 102001

Given no detection, we set the all-sky all-frequency upper limits on the GWB effective strain*:

$$h(f, \hat{\mathbf{n}}) = \sqrt{\mathscr{P}(f, \hat{\mathbf{n}})\, df}$$

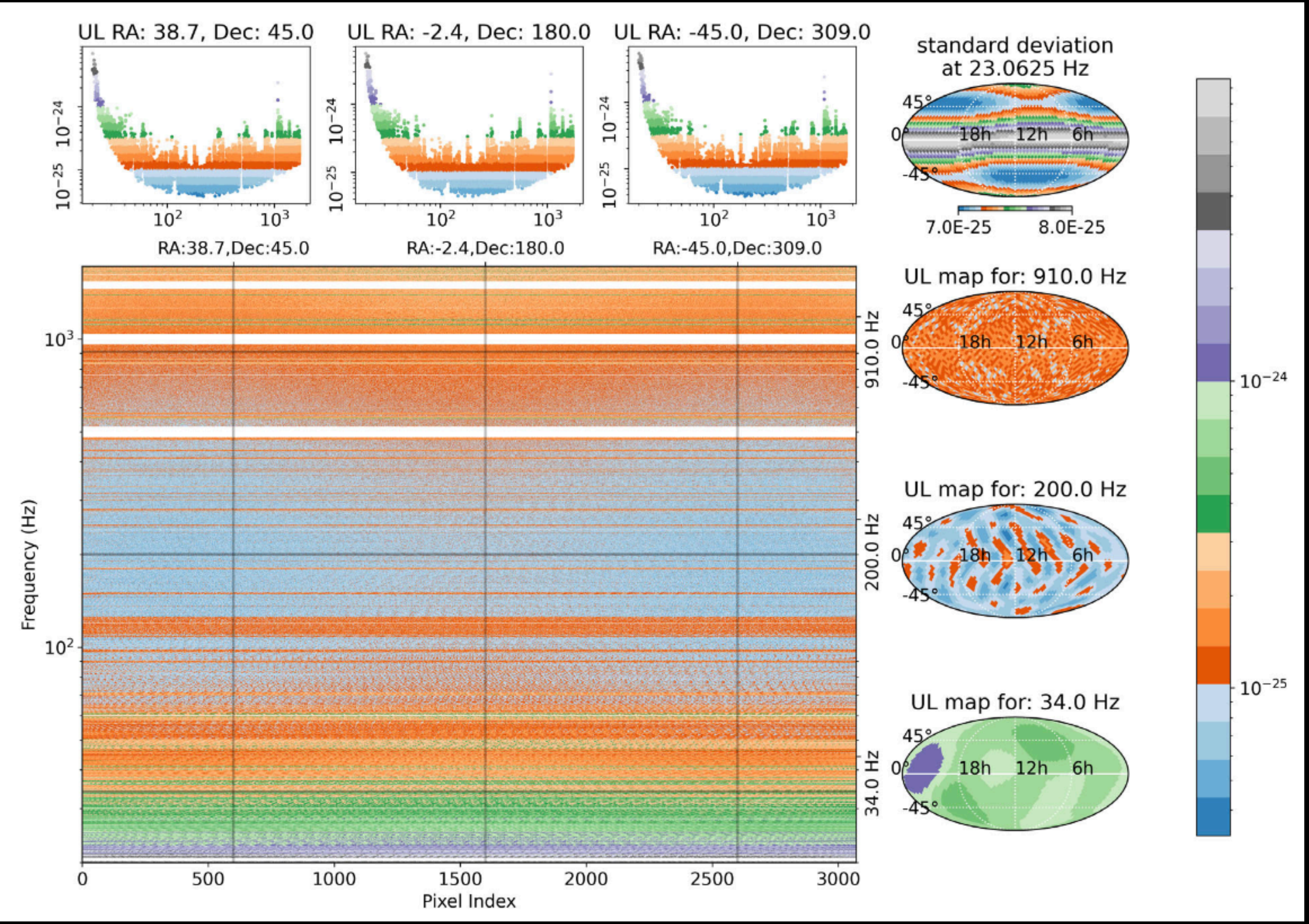

- The colour bar here denotes the range of upper limit variations.
- The vertical cross-section in this diagram shows the frequency-dependent upper limit in a particular direction.
- The Horizontal cross-sections form a map of upper limits in a particular frequency.
- Notched frequencies in a baseline appear as horizontal white bands in the plot.

*circular polarisation without Doppler correction

ALL-SKY ALL-FREQUENCY RESULTS

Phys.Rev.D 105 (2022) 10, 102001

Assume a power law and combine these narrowband maps to obtain the 'usual' broadband results

$$\hat{\mathscr{P}}(\hat{\mathbf{n}}) = \frac{\sum_f \hat{\mathscr{P}}(f,\hat{\mathbf{n}})\,\sigma_{\hat{\mathbf{n}}}^{-2}(f)\,H(f)}{\sum_f \sigma_{\hat{\mathbf{n}}}^{-2}(f)\,H^2(f)}$$

$$\sigma_{\hat{\mathbf{n}}} = \left[\sum_f \sigma_{\hat{\mathbf{n}}}^{-2}(f)\,H^2(f)\right]^{-1/2}$$

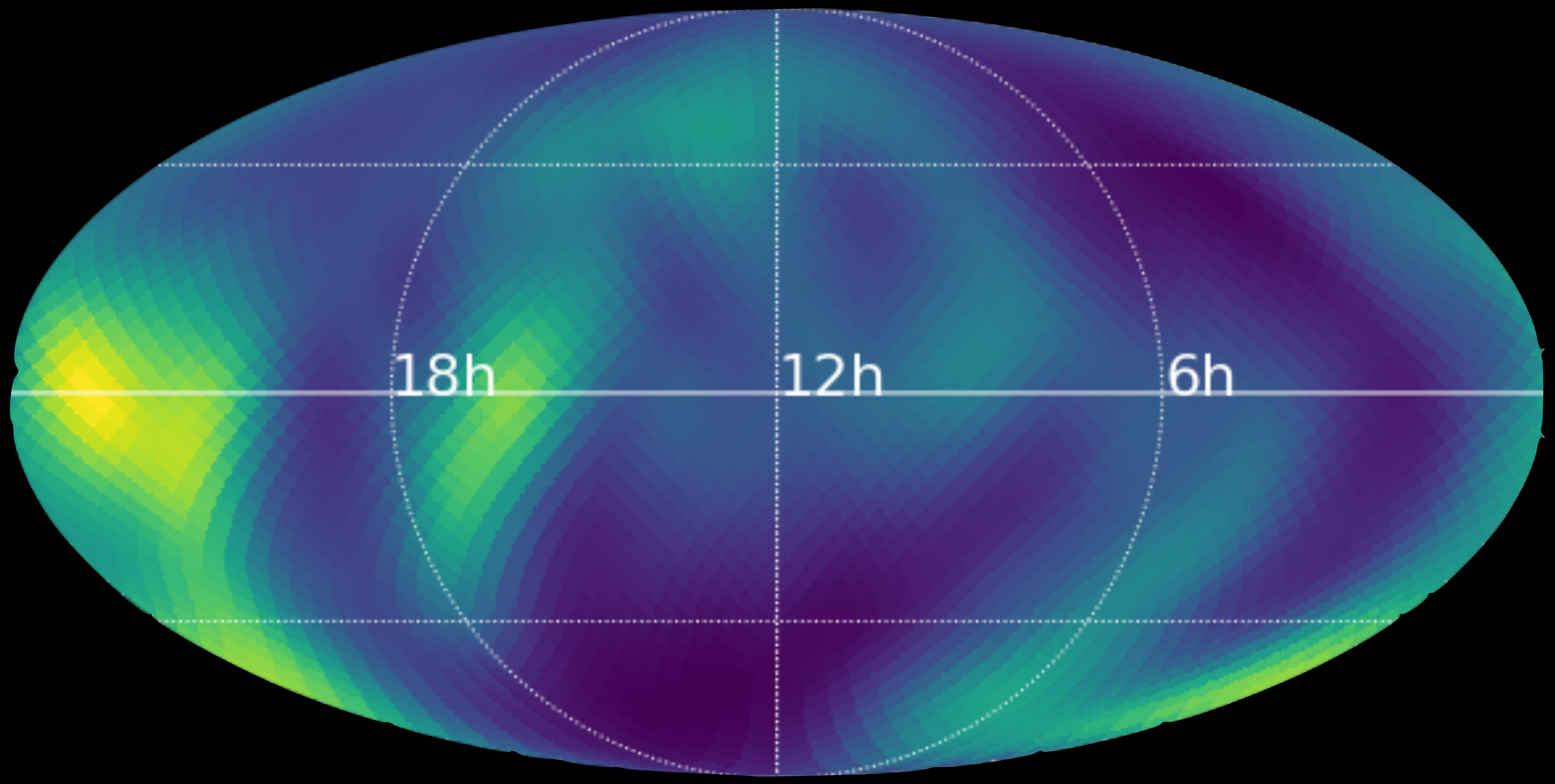

$\alpha = 0$, spectral shape

Assume a power law and sum over all the directions of these narrowband maps to obtain the 'usual' isotropic results

$$\hat{\mathscr{P}}_{\rm iso}(f)\,\sigma_{\rm iso}^{-2}(f) = \frac{5}{4\pi}\int d\hat{\mathbf{n}}\,\hat{\mathscr{P}}(f,\hat{\mathbf{n}})\,\sigma_{\hat{\mathbf{n}}}^{-2}(f)$$

$$\sigma_{\rm iso}^{-2}(f) = \left(\frac{5}{4\pi}\right)^2 \int d\hat{\mathbf{n}} \int d\hat{\mathbf{n}}'\,\Gamma_{\hat{\mathbf{n}},\hat{\mathbf{n}}'}(f)$$

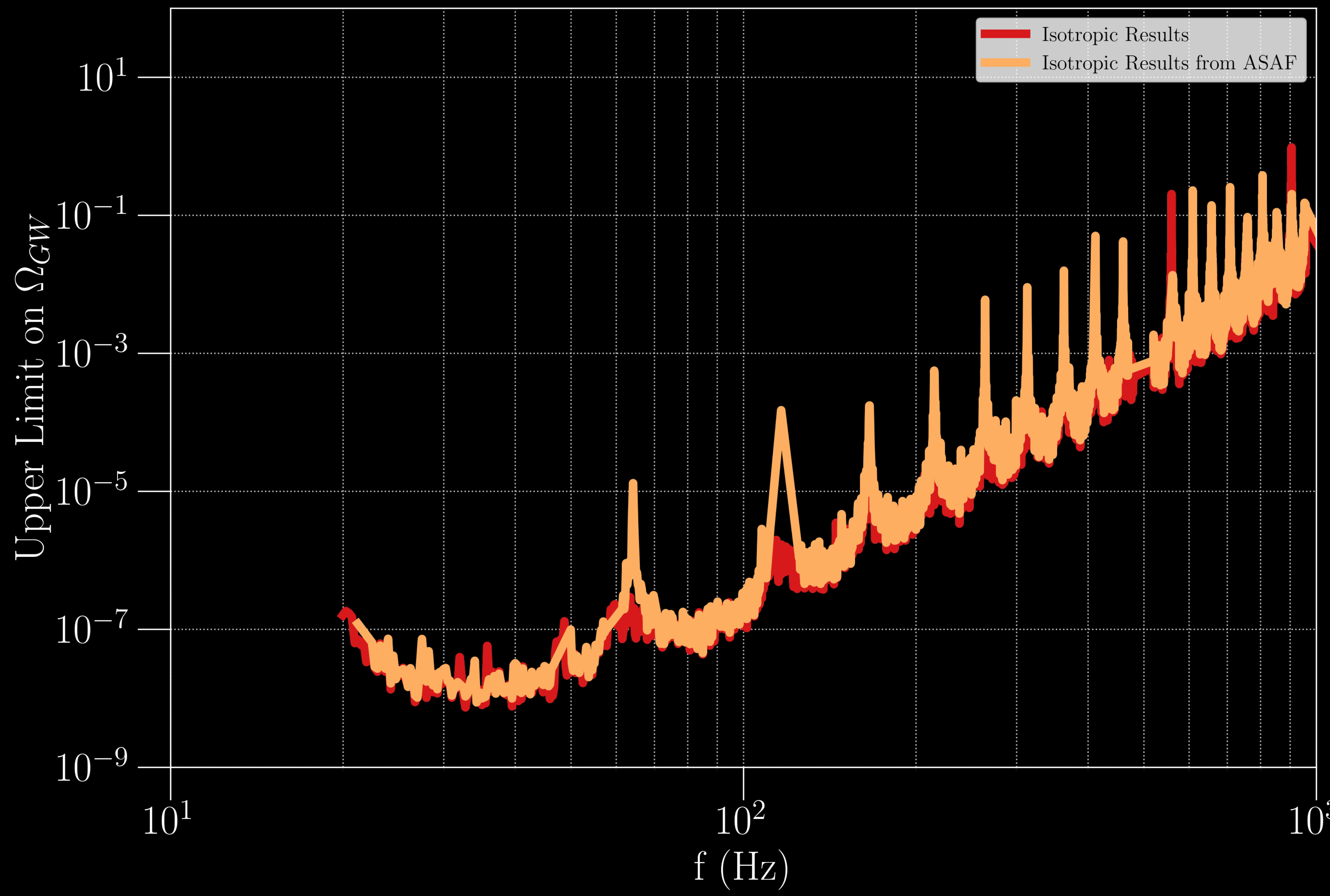

- New searches and techniques are opening up efficient ways to probe the dark universe.
- Many assumptions we consider may fail in the coming years!
    - Weak-signal limit, polarized background, non-gaussianity, non-stationarity…
- Plenty more work to do!
    - More detectors, More signals, More systems, and Dealing with real data…..

Stay tuned for the most up-to-date GWB search results from LIGO-Virgo-KAGRA collaboration in the coming months!

- New searches and techniques are opening up efficient ways to probe the dark universe.
- Many assumptions we consider may fail in the coming years!
  - Weak-signal limit, polarized background, non-gaussianity, non-stationarity…
- Plenty more work to do!
  - More detectors, More signals, More systems, and Dealing with real data…..

Stay tuned for the most up-to-date GWB search results from LIGO-Virgo-KAGRA collaboration in the coming months!

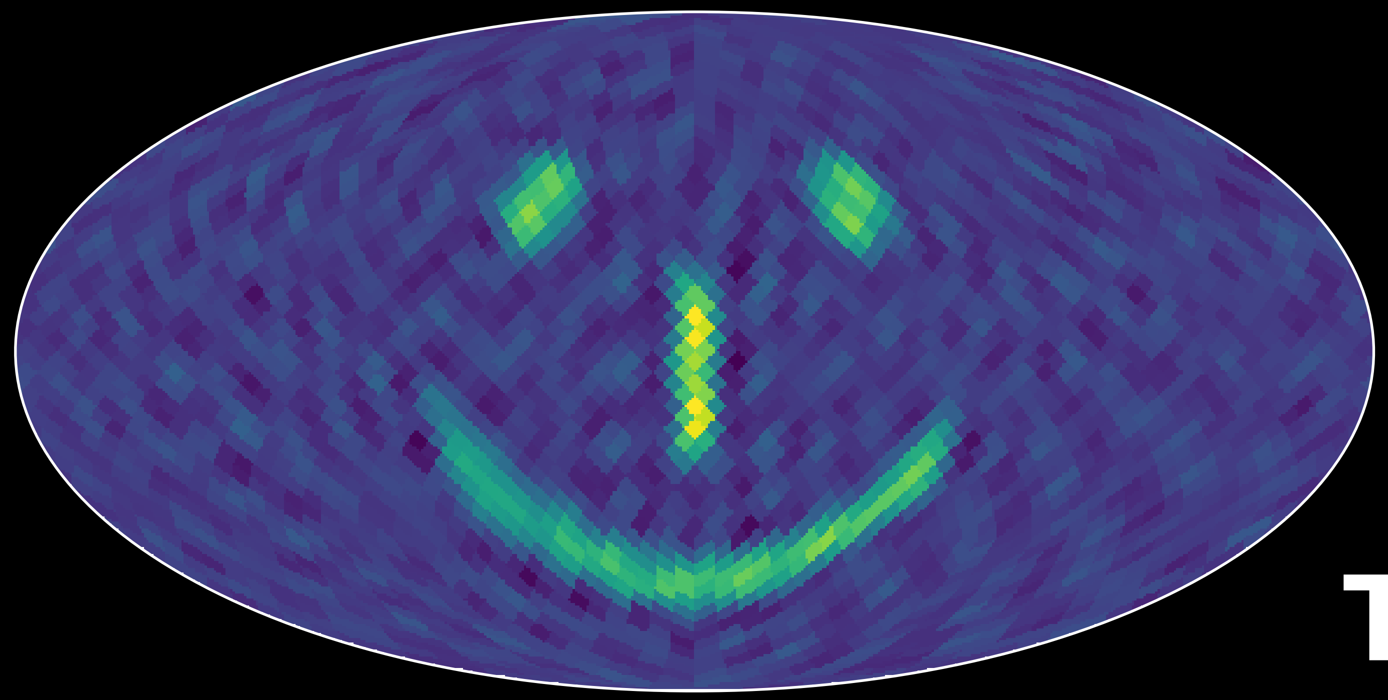

Thank you!

OVERLAP REDUCTION FUNCTION

N. Christensen: PRD 46, 5250-5266 (1992)

Detectors in different locations and with different orientations respond differently to a passing GW.

Overlap function encodes reduction in sensitivity of a cross-correlation analysis due to separation and misalignment of the detectors.

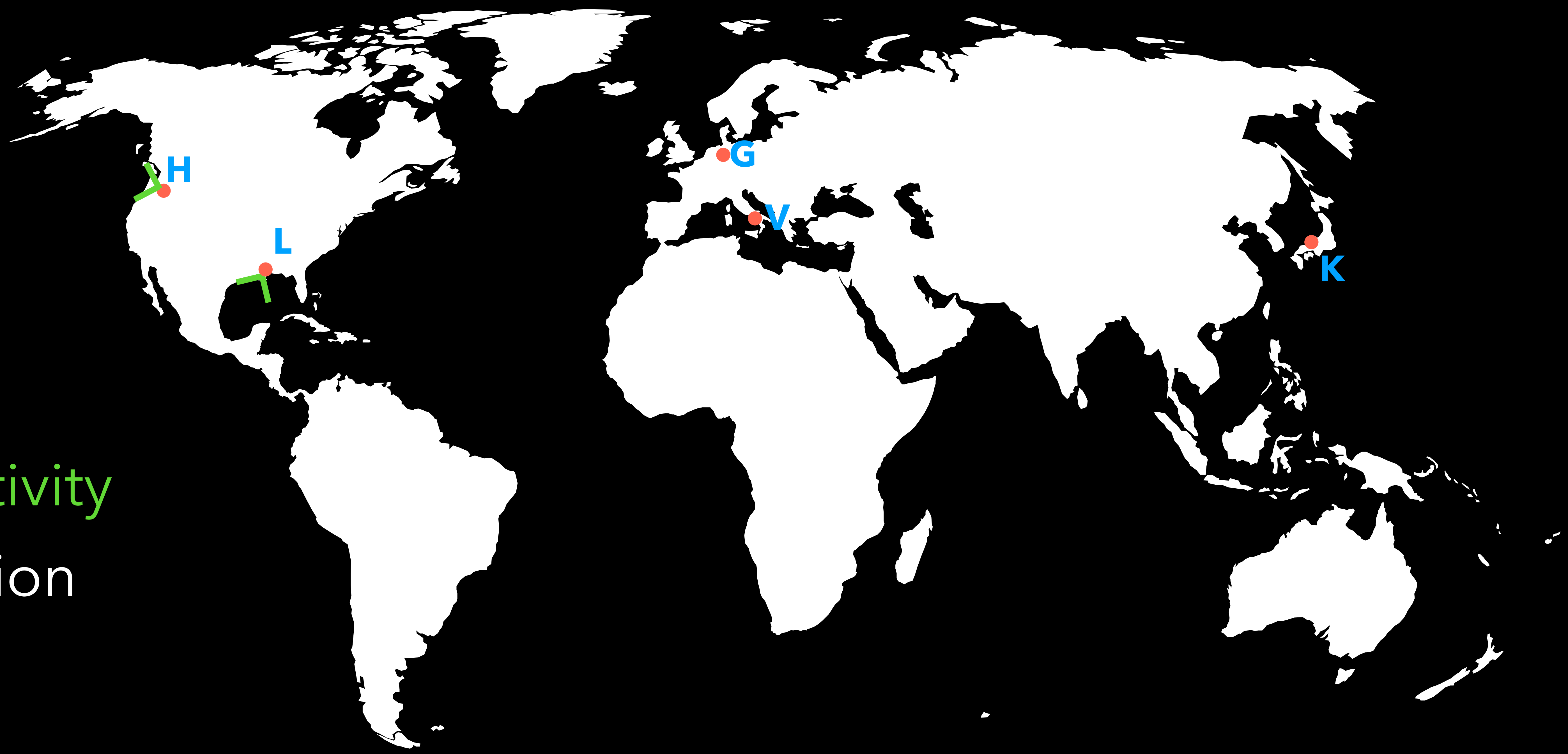

$$\gamma^{IJ}_{ft,p} = \sum_A F^A_I(\hat{\Omega}, t)\, F^A_J(\hat{\Omega}, t)\, e^{2\pi i f \hat{\Omega}\cdot\mathbf{\Delta x}_{\mathcal{I}}(t)/c}$$

OVERLAP REDUCTION FUNCTION